THE JOURNAL OF BIOLOGICAL CHEMISTRY VOL. 284, NO. 47, pp. 32507–32521, November 20, 2009

Complex Phosphatase Regulation of Ca^{2+}-activated Cl^- Currents in Pulmonary Arterial Smooth Muscle Cells*

Received for publication, July 30, 2009, and in revised form, September 4, 2009 Published, JBC Papers in Press, September 18, 2009, DOI 10.1074/jbc.M109.050401

Ramon Ayon[‡1,2], William Sones[§2], Abigail S. Forrest[‡], Michael Wiwchar[‡], Maria L. Valencik[¶], Amy R. Sanguinetti[‡], Brian A. Perrino[‖], Iain A. Greenwood[§], and Normand Leblanc[‡3]

From the Departments of [‡]Pharmacology, [‖]Physiology and Cell Biology, and [¶]Biochemistry, Center of Biomedical Research Excellence, University of Nevada School of Medicine, Reno, Nevada 89557 and the [§]Division of Basic Medical Sciences, St. George's, University of London, London SW17 0RE, United Kingdom

The present study was undertaken to determine whether the two ubiquitously expressed Ca^{2+}-independent phosphatases PP1 and PP2A regulate Ca^{2+}-activated Cl^- currents ($I_{Cl(Ca)}$) elicited by 500 nM $[Ca^{2+}]_i$ in rabbit pulmonary artery (PA) myocytes dialyzed with or without 3 mM ATP. Reverse transcription-PCR experiments revealed the expression of PP1α, PP1β/δ, PP1γ, PP2Aα, PP2Aβ, PP2Bα (calcineurin (CaN) Aα), and PP2Bβ (CaN Aβ) but not PP2Bγ (CaN Aγ) in rabbit PA. Western blot and immunofluorescence experiments confirmed the presence of all three PP1 isoforms and PP2A. Intracellular dialysis with a peptide inhibitor of calcineurin (CaN-AIP); the non-selective PP1/PP2A inhibitors okadaic acid (0.5, 10, or 30 nM), calyculin A (10 nM), or cantharidin (100 nM); and the selective PP1 inhibitor NIPP-1 (100 pM) potently antagonized the recovery of $I_{Cl(Ca)}$ in cells dialyzed with no ATP, whereas the PP2A-selective antagonist fostriecin (30 or 150 nM) was ineffective. The combined application of okadaic acid (10 nM) and CaN-autoinhibitory peptide (50 μM) did not potentiate the response of $I_{Cl(Ca)}$ in 0 ATP produced by maximally inhibiting CaN or PP1/PP2A alone. Consistent with the non-additive effects of either classes of phosphatases, the PP1 inhibitor NIPP-1 (100 pM) antagonized the recovery of $I_{Cl(Ca)}$ induced by exogenous CaN Aα (0.5 μM). These results demonstrate that $I_{Cl(Ca)}$ in PA myocytes is regulated by CaN and PP1 and/or PP2A. Our data also suggest the existence of a functional link between these two classes of phosphatases.

The activity of Ca^{2+}-activated Cl^- (Cl_{Ca})[4] channels in smooth muscle cells is enhanced by a rise in intracellular Ca^{2+} concentration $[Ca^{2+}]_i$ that occurs during stimulation by a contractile agonist. In vascular myocytes, it is thought that activation of Cl_{Ca} causes membrane depolarization due to the fact that Cl^- is actively transported into the cell (1), thus yielding an equilibrium potential (~−20 mV) that is more positive than the resting potential of the cell (~−50 mV). The ensuing depolarization caused by net Cl^- efflux from the cell through Cl_{Ca} in turn increases the open probability of voltage-dependent Ca^{2+} channels, favoring Ca^{2+} entry and increased muscle tone (2, 3). Studies of the past decade have shown that Cl_{Ca} channels of airway and arterial smooth muscle cells are down-regulated by at least one phosphorylation step involving calmodulin-dependent protein kinase II (CaMKII) (4, 5). The target of CaMKII mediating this effect is presently unknown because the molecular identity of the channel underlying Cl_{Ca} in smooth muscle and many other cell types is still unresolved. It is thought that CaMKII-mediated phosphorylation may serve as a braking system to counteract or minimize the impact of the positive feedback loop established by the Cl_{Ca}-induced depolarization, its effect on Ca^{2+} entry through L-type Ca^{2+} channels, and finally activation of Cl_{Ca} (3, 6).

In rabbit pulmonary arterial myocytes from large conduit arteries, Cl_{Ca} channel activity runs down quickly over 5–10 min of cell dialysis with 3 mM ATP to support phosphorylation (6). In contrast, when ATP is either absent or replaced by an equivalent concentration of the non-hydrolyzable ATP analogue, AMP-PNP, rundown is attenuated and is followed by a progressive recovery of the current (6). These observations are consistent with the idea that phosphorylation by CaMKII and perhaps other kinases overwhelms the activity of phosphatases whose activity can be unmasked by lack of substrate or a substrate that cannot be hydrolyzed. This hypothesis is also supported by recent studies from our group showing that in rabbit pulmonary artery myocytes dialyzed with ATP, Cl_{Ca} rundown could be similarly attenuated and subsequently reversed by cellular introduction of a constitutively active form of calcineurin (CaN) (7), a serine-threonine Ca^{2+}-dependent phosphatase also referred to as PP2B. Endogenous CaN activity also antag-

* This work was supported, in whole or in part, by National Institutes of Health Grant 5 RO1 HL 075477. This work was also supported by British Heart Foundation Grants PG/05/038 (to I. A. G.). This work was also made possible by National Institutes of Health, National Center for Research Resources, Grants NCRR 5 P20 RR15581 (to N. L.), NCRR 5 P20 RR15581 and 5 PPG HL 76611 (to M. L. V.), and NCRR 5 P20 RR018751 (to B. A. P.), supporting two Centers of Biomedical Research Excellence at the University of Nevada School of Medicine (Reno, NV).

[1] Supported by National Institutes of Health Ruth L. Kirschtein Predoctoral Fellowship Award 2 F32 HL090023.

[2] Both authors contributed equally to this work.

[3] To whom correspondence should be addressed: Dept. of Pharmacology/MS 318, Center of Biomedical Research Excellence (COBRE), University of Nevada School of Medicine, Reno, NV 89557-0270. Tel.: 775-784-1420; Fax: 775-784-1620; E-mail: NLeblanc@Medicine.Nevada.edu.

[4] The abbreviations used are: Cl_{Ca}, Ca^{2+}-activated Cl^- channel; BAPTA, 1,2-bis(*o*-aminophenoxy)ethane-*N*,*N*,*N*′,*N*′-tetraacetic acid; CaN, calcineurin; CaN-AIP, calcineurin autoinhibitory peptide; CaMKII, calcium/calmodulin-dependent kinase II; CsA, cyclosporine A; I_{CaL}, L-type Ca^{2+} current; $I_{Cl(Ca)}$, Ca^{2+}-activated Cl^- current; I-V, current-voltage relationship; OA, okadaic acid; PA, pulmonary artery; PBS, phosphate-buffered saline; $PP1_c$ and $PP2A_c$, purified catalytic subunits of PP1 and PP2A, respectively; TEA, tetraethylammonium chloride; AMP-PNP, 5′-adenylyl-β,γ-imidodiphosphate; ANOVA, analysis of variance.

onizes CaMKII-induced suppression of Cl_{Ca} activity in rabbit pulmonary (7, 8) and coronary (9) artery myocytes.

The major goal of the present study was to determine whether the two ubiquitously expressed serine-threonine phosphatases PP1 (protein phosphatases type 1) and PP2A (protein phosphatases type 2A) might also regulate Cl_{Ca} in pulmonary arterial myocytes. Such a premise was partially based on the observation that in coronary myocytes, CaN-mediated up-regulation of the Ca^{2+}-activated Cl^- current ($I_{Cl(Ca)}$) was Ca^{2+}-dependent, displaying a significant contribution of this phosphatase at intermediate $[Ca^{2+}]_i$ (350 and 500 nM) but not at high $[Ca^{2+}]_i$ (1 μM) (9). At such high levels of $[Ca^{2+}]_i$, inhibition of CaMKII with KN-93 after suppressing CaN with cyclosporine A (CsA) still led to enhancement of $I_{Cl(Ca)}$ (9), suggesting the involvement of another phosphatase. Our study shows that as for CaN (7, 9), several isoforms of PP1 and PP2A are expressed at the mRNA and protein levels in rabbit pulmonary artery, and these Ca^{2+}-independent phosphatases play a major role in regulating these channels.

EXPERIMENTAL PROCEDURES

Smooth Muscle Cell Dispersion Technique—Single smooth muscle cells were isolated by a method similar to that previously used by our group (4, 6, 7). In brief, cells were prepared from the main and secondary pulmonary arterial branches dissected from New Zealand White rabbits (2–3 kg) killed by anesthetic overdose in accordance with British and American guidelines for animal care. After dissection and removal of connective tissue, the pulmonary arteries were cut into small strips and incubated overnight (~16 h) at 4 °C in a low Ca^{2+} physiological salt solution (see composition below) containing either 10 or 50 μM $CaCl_2$ and ~0.2–0.5 mg ml^{-1} papain, 0.15 mg ml^{-1} dithiothreitol, and 2 mg ml^{-1} bovine serum albumin. The next morning, the tissue strips were rinsed three times in low Ca^{2+} PSS and incubated in the same solution for 10 min at 37 °C. Cells were released by gentle agitation with a wide bore Pasteur pipette and then stored at 4 °C until used (within 10 h following dispersion).

Patch Clamp Electrophysiology—Ca^{2+}-activated Cl^- currents were elicited using the conventional whole-cell configuration of the patch clamp technique with a pipette solution containing either 0 or 3 mM ATP. The pipette solution also contained 10 mM BAPTA as the Ca^{2+} buffer, and free $[Ca^{2+}]$ was set to 500 nM by the addition of 7.08 mM $CaCl_2$. Each desired free $[Ca^{2+}]$ was estimated by the calcium chelator program MaxC (version 2.50; available on the Stanford web site). Using a Ca^{2+}-sensitive electrode and calibrated solutions, the total amounts of $CaCl_2$ and $MgCl_2$ added were calculated by the software to yield accurate free Ca^{2+} concentration with both EGTA and BAPTA (6, 7, 9). Contamination of $I_{Cl(Ca)}$ from other types of current was minimized by the use of CsCl and tetraethylammonium chloride (TEA) in the pipette solution and TEA in the external solution. On any given experimental day, pipette solutions containing one or more drugs were rigorously alternated with one lacking the substance(s). Data for each group were collected in cells from at least two animals but generally more.

$I_{Cl(Ca)}$ was evoked immediately upon rupture of the cell membrane, and the voltage-dependent properties were monitored every 10 s (Figs. 3–5, 7, 8*B* (*b*), and 9) or 20 s (Figs. 6 and 8 (*A* and B (*a*)) by stepping from a holding potential of −50 mV to +90 mV for 1 s, followed by repolarization to −80 mV for 1 s. Current-voltage (I-V) relationships were constructed by stepping in 10-mV increments from holding potential to test potentials between −100 mV and +130 mV for 1 s after 20 min dialysis. For I-V relationships, $I_{Cl(Ca)}$ was expressed as current density (pA/picofarads) by dividing the amplitude of the current measured at the end of the voltage clamp step by the cell capacitance. For all figure panels showing a time course of $I_{Cl(Ca)}$ changes, the late current measured at +90 mV was normalized to the amplitude of first current elicited at time 0 (~30 s after breaking the seal and measuring cell capacitance).

Solutions and Reagents—Single pulmonary artery smooth muscle cells were isolated by incubating pulmonary artery tissue strips in the following low Ca^{2+} physiological salt solution: 120 mM NaCl, 4.2 mM KCl, 25 mM $NaHCO_3$ (pH 7.4 after equilibration with 95% O_2, 5% CO_2 gas), 1.2 mM KH_2PO_4, 1.2 mM $MgCl_2$, 11 mM glucose, 25 mM taurine, 0.01 mM adenosine, and 0.01 or 0.05 mM $CaCl_2$. The K^+-free bathing solution used in all patch clamp experiments had the following composition: 126 mM NaCl, 10 mM Hepes-NaOH (pH 7.35), 8.4 mM TEA, 20 mM glucose, 1.2 mM $MgCl_2$, and 1.8 mM $CaCl_2$. The pipette solution had the following composition: 20 mM TEA, 106 mM CsCl, 10 mM Hepes-CsOH (pH 7.2), 10 mM BAPTA, 0 or 3 mM ATP, and 0.2 mM GTP. To this solution, the following total amounts of $CaCl_2$ and $MgCl_2$ were added to set free $[Mg^{2+}]$ to 0.5 mM and free $[Ca^{2+}]$ to 500 nM: 7.08 mM $CaCl_2$, 3.0 mM $MgCl_2$ (with 3 mM ATP disodium salt and 500 nM Ca^{2+}); 7.08 $CaCl_2$, 0.545 $MgCl_2$ (with no ATP and 500 nM Ca^{2+}). All enzymes and analytical grade reagents were purchased from Sigma. Drugs and peptides were purchased from the following sources: okadaic acid, Sigma; cyclosporine A, LC Laboratories (Woburn, MA); calyculin A, Merck; calcineurin, EMB Biosciences (San Diego, CA); fostriecin, A. G. Scientific (San Diego, CA); calcineurin autoinhibitory peptide (CaN-AIP), Biomol (Plymouth Meeting, PA); purified constitutively active forms of PP1 and PP2A and NIPP-1 (nuclear inhibitory peptide of protein phosphatase type 1), Merck.

Detection of PP1, PP2A, and PP2B mRNA Expression by Reverse Transcription-PCR—mRNA was isolated from homogenates of whole rabbit pulmonary artery, rabbit brain, and mouse brain using PureZol (Bio-Rad). Prior to preparing cDNA, the RNA was treated with DNase I (Invitrogen) to prevent genomic DNA contamination. The cDNA was prepared using oligo(dT) and dNTP mixtures with Superscript II, with a negative reverse transcriptase control prepared for each tissue sample (Invitrogen). Rabbit sequences were available for glyceraldehyde-3-phosphate dehydrogenase, CaNβ, and CaNγ, and PCR primers were designed accordingly. For all of the other enzymes (PP1α, PP1β/δ, PP1γ, PP2Aα, PP2Aβ, and CaN Aα), no rabbit sequences were available, and degenerate PCR primers were thus designed and generated against an alignment of the sequences available for mouse, rat, and human. A separate mouse glyceraldehyde-3-phosphate dehydrogenase primer pair was also designed. All primers were synthesized by Operon

Biotechnologies (Huntsville, AL). Amplification of the cDNA was performed using Gotaq (Promega, Madison, WI), which had an amplification profile consisting of an initial step to 95 °C for 2 min to activate the Amplitaq polymerase, followed by 36 cycles of denaturation at 95 °C for 30 s, annealing at T_a (in °C; the optimal annealing temperature for each primer pair; range: 60–63 °C) for 30 s, and extension at 72 °C for 30 s, followed by a final extension step at 72 °C for 5 min. The amplified products (10 μl) were separated by electrophoresis on a 2% agarose/Tris, acetic acid, EDTA gel, and the DNA bands were visualized by ethidium bromide staining. Both a negative reverse transcription control (described above) and a non-template control for the master mix of reagents made for each primer pair were run on the gels to ensure lack of contaminants in the samples. In addition, glyceraldehyde-3-phosphate dehydrogenase reactions were run as a positive control for all cDNA samples used. Once DNA bands were observed at approximately the appropriate size, the remainders of the PCR samples were sent for sequencing, and the sequences obtained were searched against the NCBI Blast data base to confirm the identity of the products.

Western Blot Analysis of PP1 and PP2A—100 or 150 μg of protein from the 1000 × *g* supernatant of homogenized rabbit pulmonary artery (PA) smooth muscle and 50 or 75 g of protein from the 1000 × *g* supernatant of homogenized rabbit brain were separated by SDS-PAGE (10%) and electroblotted onto nitrocellulose membranes. Protein concentrations were determined by the Bradford assay using bovine γ-globulin as a standard. The blots were probed with Santa Cruz Biotechnology, Inc. (Santa Cruz, CA) goat anti-PP1α, -PP1β/δ, -PP1γ, or -PP2A antibodies (1:8000 dilution), followed by a horseradish peroxidase-conjugated rabbit anti-goat IgG (1:50,000 dilution) antibody. Immunodetection was carried using ECL Advance from Amersham Biosciences, and the TIFF images were collected with a CCD camera imaging system (Labworks, UVP Inc.). The collected TIFF images were analyzed using Adobe Photoshop.

Immunocytochemistry and Confocal Imaging—Freshly isolated rabbit pulmonary artery smooth muscle cells were fixed in 3.7% formaldehyde at room temperature for 15 min and then permeabilized with 0.1% Triton X-100 (Sigma) in phosphate-buffered saline (PBS; EMD Biosciences, CA). The cells were washed thoroughly in PBS before being cytospun (600 rpm/5 min) onto slides coated with poly-L-lysine (10 μg/ml; Sigma). All cells were blocked for 1 h in 1% bovine serum albumin (Roche Applied Science) at room temperature before being incubated with primary goat polyclonal antibodies (PP1α, PP1β/δ, PP1γ, or PP2A; Santa Cruz Biotechnology, Inc.; 1:50) for 1 h at room temperature. After washing in PBS, the cells were further incubated with biotinylated anti-goat IgG (1:100; Vector Laboratories) and the nuclear stain bisbenzamide (1:500; Biomol) to facilitate cell identification. After further washing with PBS, the cells were incubated for another 30 min with streptavidin (1:1000; Molecular Probes, Eugene, OR), washed with PBS, and mounted onto coverslips using Gel/Mount anti-fade medium (Biomeda). Control slides were also processed using the secondary antibodies only. Rabbit pulmonary artery myocytes were viewed using a Plapon ×60 oil objective on an Olympus IX81 microscope coupled to an Olympus Fluoview FV1000 confocal scanning system equipped with image acquisition and analysis software (Olympus Fluoview F1000). 405 and 594 nm laser lines were used to visualize the bisbenzamide and streptavidin-conjugated secondary antibodies, respectively. All images shown in Fig. 2 were normalized to identical contrast and brightness settings by Olympus Fluoview F1000 software, and individual images were exported as JPEG files into CorelDraw 12 (Corel Corp., Ottawa, Canada).

Synthesis of Constitutively Active Calcineurin—Constitutively active calcineurin Aα isoforms were synthesized by introducing stop codons into the cDNA for the catalytic subunit, CaN A, causing the translated CaN A subunits to truncate immediately C-terminal of the CaM-binding domain and delete the autoinhibitory domain, so the autoinhibitory domain was deleted. All methodologies for cDNA manipulation, baculovirus screening, and purification of CaN using monolayer cultures of Sf 21 cells have been described previously (7, 10–12).

Statistical Analysis—All data were pooled from *n* cells taken from at least two different animals, with *error bars* representing the S.E. In some experiments, $I_{Cl(Ca)}$ was recorded with a drug-free pipette solution, which was alternated within the same day with one containing a drug, a peptide inhibitor, or a phosphatase of interest. This strategy was employed to attenuate cell response variability due to phenotypic variations arising from different animals. All data were first pooled in Excel, and means ± S.E. were exported to Origin version 7.5 software (OriginLab Corp., Northampton, MA) for plotting and curve fitting. All graphs and current traces were exported to CorelDraw 12 (Corel Corp.) for final processing of the figures. The data were analyzed with either the unpaired Student's *t* test to evaluate the statistical significance between the means of two groups or one-way ANOVA test followed by Bonferroni *post hoc* multiple range tests in multiple group comparisons (Origin version 7.5 software, OriginLab Corp.). $p < 0.05$ was considered to be statistically significant.

RESULTS

Multiple Isoforms of PP1, PP2A, and PP2B Are Expressed in the Rabbit Pulmonary Artery—Reverse transcriptase polymerase chain reaction experiments revealed significant expression in the rabbit PA for PP1α, PP1β/δ, PP1γ, PP2Aα, PP2Aβ, PP2Bα (CaN Aα), and PP2Bβ (CaN Aβ) but not PP2Bγ (CaN Aγ) (Fig. 1*A*). All isoforms were confirmed by bidirectional sequencing. Western blot analysis performed on tissue homogenates from the rabbit pulmonary artery and brain (which served as a positive control) detected the presence of PP1α, PP1β/δ, PP1γ, and PP2A (Fig. 1*B*), all of appropriate sizes for these isoforms with a molecular mass ranging from 35 to 37 kDa (13, 14). Previous Western blot analysis in the rabbit pulmonary artery had revealed expression of both CaN Aα and CaNAβ (7). The PP1 and PP2A antibodies used for Western blots were also used in immunocytochemistry experiments to immunostain the three PP1 isoforms and PP2A. Confocal imaging revealed strong and uniform cytoplasmic labeling of PP1α (Fig. 2*A*) and PP1γ (Fig. 2*C*). Although faint, significant levels of immunofluorescence above those observed for cells exposed to secondary antibody alone (Fig. 2*E*) were detectable for PP1β/δ (Fig. 2*B*) and PP2A (Fig. 2*D*). These results demonstrate the expression

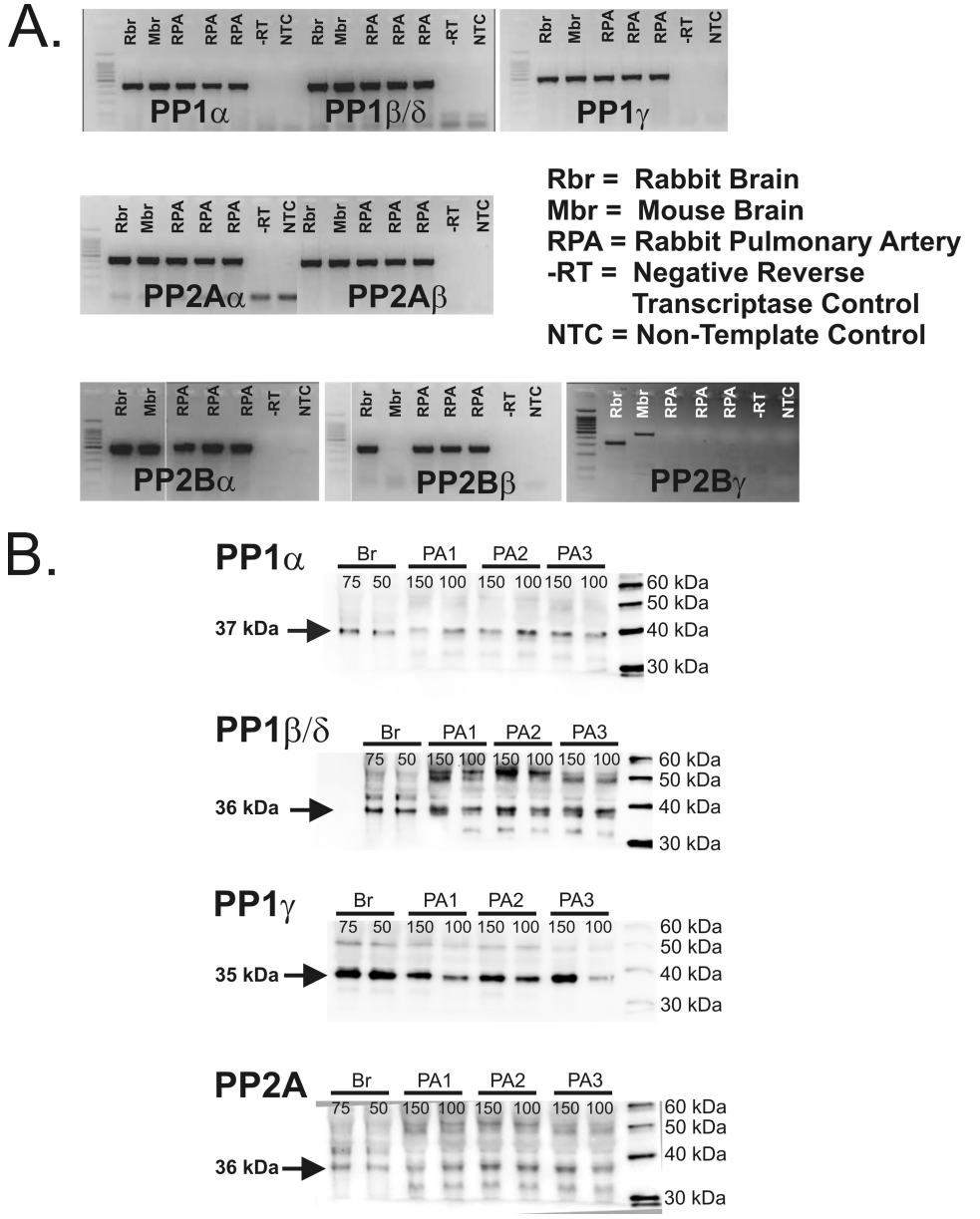

FIGURE 1. **Detection of multiple isoforms for PP1, PP2A, and PP2B in the rabbit pulmonary artery.** *A*, reverse transcription-PCR revealed significant expression in the rabbit pulmonary artery for PP1α, PP1β/δ, PP1γ, PP2Aα, PP2Aβ, PP2Bα, and PP2Bβ but not PP2Bγ. *B*, Western blot analysis performed on tissue homogenates from rabbit pulmonary artery. Homogenates from rabbit brain served as a positive control. These data revealed the presence of PP1α, PP1β/δ, PP1γ, and PP2A (isoform-specific antibodies were not available for PP2A). The *number above* each *lane* represents the amount of protein loaded in μg.

in the rabbit PA of several transcripts encoding for multiple isoforms of PP1, PP2A, and PP2B, which were correlated by the expression of similar PP1 (this study) and PP2B (7) protein isoforms. Finally, PP2A was also recognized at the protein level by a general PP2A antibody.

Impact of General Phosphorylation Status on $I_{Cl(Ca)}$—Fig. 3 shows the basic premise under which the functional part of the study allowed us to study the impact of PP1 and PP2A. Fig. 3*A* shows representative traces of $I_{Cl(Ca)}$ evoked by the bottom protocol in two different myocytes and recorded at different times following seal rupture. One was dialyzed with 3 mM ATP (*left traces*) and the other with no ATP (*right traces*). Similar to our previous studies (6, 7), both the time-dependent outward relaxation at +90 mV and inward tail current at −80 mV declined substantially over the course of 20 min when the pipette solution contained 3 mM ATP. In contrast, the current recorded after 5 min in the absence of ATP exhibited less rundown and eventually began to increase over the following 15 min to reach a level that exceeded the initial current recorded at $t = 0$ (0 ATP; *bottom trace*).

Fig. 3*B* shows a summary of similar experiments where late $I_{Cl(Ca)}$ at +90 mV was normalized against the current measured at $t = 0$ and plotted as a function of time. The *three arrows above* the *plots* indicate the time points during which the recordings in Fig. 3*A* were taken for guidance. In these experiments, fully activated $I_{Cl(Ca)}$ decreased to ~35% of its initial level and slightly recovered to about 40% of the initial level after 20 min. Cell dialysis with a solution lacking ATP led to effects on $I_{Cl(Ca)}$ similar to that produced by replacement of ATP with AMP-PNP (6). The current ran down to about 75% of the initial current level but then began to recover after 3–4 min to equal the initial current amplitude after 15 min and then exceed it by ~10% after 20 min. Another interesting aspect of the impact of phosphorylation on Cl_{Ca} channel gating relates to the progressive changes in kinetics of the current during cell dialysis, as shown in Fig. 3*A*. With 3 mM ATP, the time constant τ of activation of $I_{Cl(Ca)}$ at +90 mV progressively increased from 268 ms after seal rupture to 352 and 760 ms after 5 and 20 min of cell dialysis, respectively; the time constant of deactivation at −80 mV followed an opposite trend decreasing from 134 ms at $t = 0$, to 122 ms and 117 ms after 5 and 20 min, respectively. In the absence of ATP, the time constants of activation and deactivation displayed a transient behavior. The time constant of activation at +90 mV increased from 228 ms at $t = 0$–483 ms after 5 min but then declined to 226 ms after 20 min; the time constant of deactivation exhibited a similar trend in the opposite direction, with a value of 104 ms after breaking the seal and 93 ms and 116 ms after 5 and 20 min. These changes are consistent with the reported phosphorylation-induced alterations in gating (6, 7, 9). At the onset of cell dialysis, one would expect the cells in both groups to be in a state of general dephosphorylation

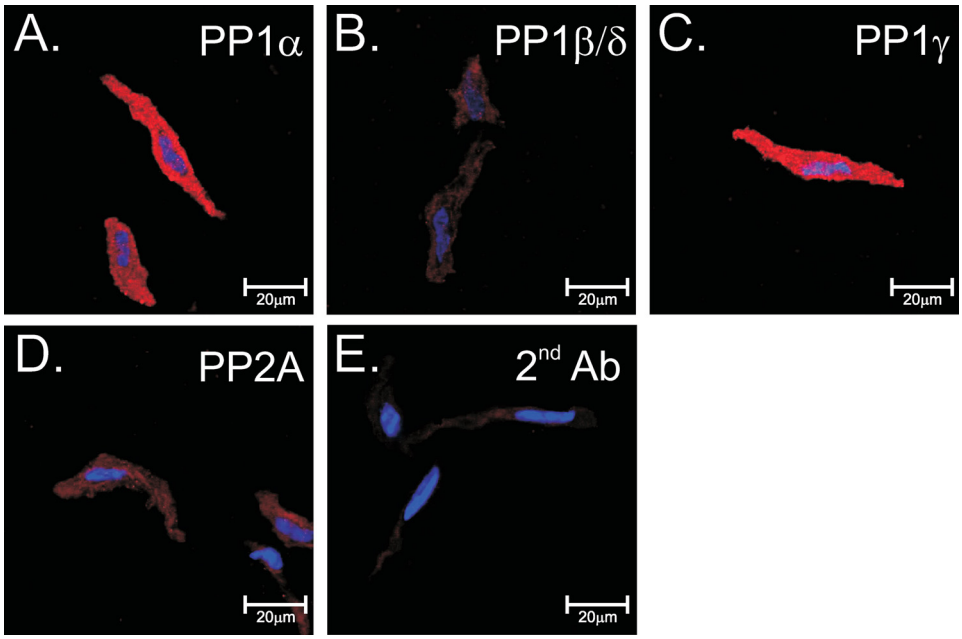

FIGURE 2. **Immunodetection of protein phosphatases in rabbit pulmonary artery smooth muscle cells.** Shown is immunolabeling of isolated cells for PP1α (*A*), PP1β/δ (*B*), PP1γ (*C*), and PP2A (*D*), all detected using a biotinylated anti-goat antibody (*red*) with streptavidin. *E*, cells labeled with secondary antibody only. For all images, nuclei were stained with bisbenzamide (*blue*). Image series were taken in the *z*-dimension at 0.5-μm intervals, and a full cross-section of the cell was selected for display purposes.

because intracellular Ca^{2+} has had time to activate the channels with little influence on CaMKII and CaN. Over time in cells dialyzed with ATP, the dominance of CaMKII over phosphatases leads to current rundown, slowed activation, and accelerated deactivation. This trend is also observed initially in the absence of ATP. $I_{Cl(Ca)}$ rundown occurs during the first 5 min, and kinetic changes follow the same pattern as cells dialyzed with ATP. These observations are in agreement with the idea that following membrane rupture, the endogenous levels of ATP combined with the rapid dialysis of high Ca^{2+} levels are sufficient to activate CaMKII and phosphorylate the channel or accessory subunit concomitant with activation of the channel. However, the progressive dialysis of a solution lacking substrate probably shifts the balance of normally dominant kinase-dependent phosphorylation to a progressive state of global dephosphorylation of target proteins by endogenous phosphatases, leading to $I_{Cl(Ca)}$ recovery and reversal of the changes in kinetics. The following series of experiments provides support to this hypothesis.

Effects of Non-selective Inhibitors of PP1 and PP2A—Okadaic acid (OA) is a tumor suppressor and widely utilized inhibitor of serine/threonine phosphatases. Although it inhibits both PP1 and PP2A with high affinity *in vitro*, biochemical assays have shown that it has ~10-fold higher affinity for blocking PP2A (PP2A, 0.04–1 nM; PP1, 3–60 nM) (15–20). We tested the effects of three concentrations of OA in an attempt to determine if Ca^{2+}-independent phosphatases regulated Cl^- channel activity and whether one isoform was more influential than the other. Again, the cells were dialyzed in the absence of ATP to induce rundown and recovery of $I_{Cl(Ca)}$ over 20 min of cell dialysis. Fig. 4*A* (*a*) shows that OA dose-dependently inhibited the recovery of late $I_{Cl(Ca)}$ at +90 mV, with 0.5 nM producing no significant effect and 30 nM causing strong inhibition to levels resembling those achieved by the highly specific CaN inhibitor CaN-AIP (see Fig. 9*A* (*a*)) or when the cells are dialyzed with 3 mM ATP (Fig. 3). Analysis of the concentration-dependent effect of OA on late $I_{Cl(Ca)}$ recorded at +90 mV revealed an IC_{50} of ~2 nM (Fig. 4*A* (*b*)). Lack of inhibition with 0.5 nM OA and potent block with 10 and 30 nM OA are also evident in Fig. 4*B*, where I-V relationships for late $I_{Cl(Ca)}$ in the absence and presence of OA are displayed.

We next examined the effects of another PP1 and PP2A inhibitor, cantharidin, which displays lower affinity than OA for reducing catalytic activity of these enzymes but, like OA, exhibits a higher selectivity for inhibiting PP2A over PP1 (PP2A, 40–200 nM; PP1, 473–2000 nM) (17, 19). As shown in Fig. 5*A*, 100 nM cantharidin dialyzed into cells supplied with no ATP enhanced the initial rundown of $I_{Cl(Ca)}$ and suppressed its delayed recovery, albeit at a lower extent than that produced by 30 nM OA (Fig. 4*A*). As for OA, the current remaining after 20 min in the presence of cantharidin displayed outward rectification and reversed near E_{Cl} (Fig. 5*B*). Overall, these data suggest that PP1 is a more important driver of Cl^- channel activity than PP2A.

Effects of Specific Inhibitors of PP1 and PP2A—Fig. 6 shows a *graph* summarizing the effects of cell dialysis with the nuclear scaffold protein NIPP-1. This agent is a highly specific polypeptide and potent endogenous inhibitor of PP1 (K_i of ~1 pM) (21), which has no effect on PP2A and calcineurin at concentrations 250-fold higher than required to block PP1. With 100 pM in the pipette solution, NIPP-1 obliterated the recovery of $I_{Cl(Ca)}$ in cells dialyzed with no ATP. Fig. 6 also shows that the inhibition achieved by NIPP-1 was similar to the level reached after rundown in the presence of 3 mM ATP. The effects of NIPP-1 were lost after denaturation at room temperature (data not shown).

We next examined the effects of a specific blocker of PP2A, fostriecin, which was again included in the pipette solution. Fostriecin is an antitumor antibiotic that inhibits PP2A activity with an IC_{50} of 3.2 nM and exhibits very weak activity on PP1 (IC_{50} = 131 μM), thus offering excellent selectivity for PP2A (20). Inclusion of 30 nM fostriecin in the pipette solution failed to alter the magnitude of $I_{Cl(Ca)}$ in the absence of ATP over a 20-min period of cell dialysis (Fig. 7*A* (*a*)). We also tested a 5-fold higher concentration (150 nM) on $I_{Cl(Ca)}$. Again, a concentration ~47-fold higher than the IC_{50} altered neither the time course of recovery of late $I_{Cl(Ca)}$ at +90 mV in the absence of ATP (Fig. 7*A* (*b*)) nor its voltage dependence (Fig. 7*B*).

Effects of Exogenous Application of Constitutively Active Forms of PP1 or PP2A—Our group has recently shown that the internal application of an active form of CaN Aα but not CaN

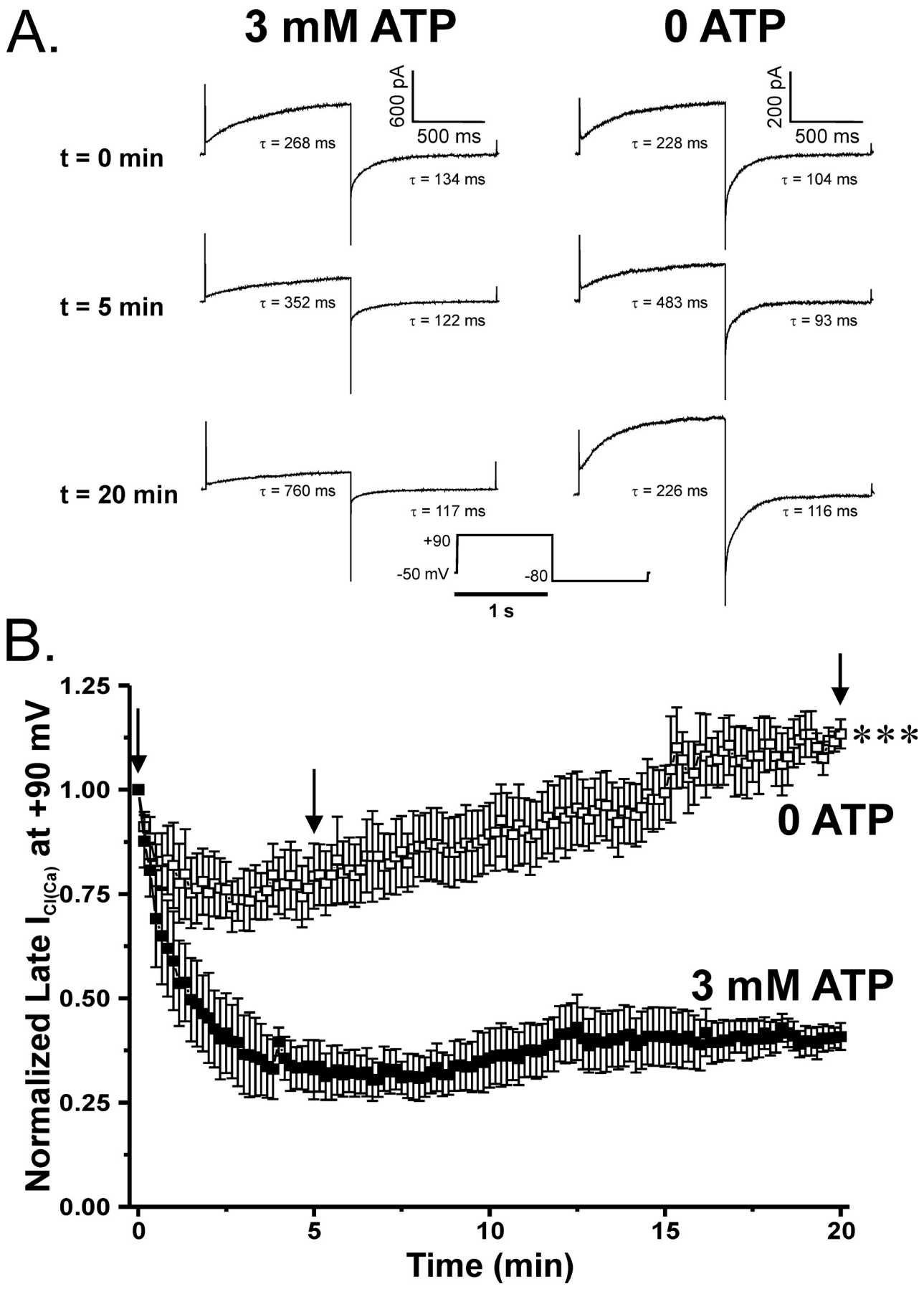
A.
3 mM ATP
0 ATP
t = 0 min
t = 5 min
t = 20 min
600 pA
500 ms
200 pA
500 ms
τ = 268 ms
τ = 134 ms
τ = 228 ms
τ = 104 ms
τ = 352 ms
τ = 122 ms
τ = 483 ms
τ = 93 ms
τ = 760 ms
τ = 117 ms
τ = 226 ms
τ = 116 ms
+90
-50 mV
-80
1 s
B.
Normalized Late $I_{Cl(Ca)}$ at +90 mV
1.25
1.00
0.75
0.50
0.25
0.00
0
5
10
15
20
Time (min)
***
0 ATP
3 mM ATP

Aβ could reverse the rundown of $I_{Cl(Ca)}$ in rabbit pulmonary myocytes dialyzed with 3 mM ATP to promote phosphorylation (7). The stimulation of $I_{Cl(Ca)}$ was annihilated by boiling the recombinant phosphatase or by dialyzing in parallel a specific peptide inhibitor of CaN. We thus employed a similar approach to examine the role of the Ca^{2+}-independent phosphatases PP1 and PP2A. Unexpectedly, Fig. 8*A* shows that inclusion of any one of three PP1 concentrations ranging from 5 to 40 units/ml, which are considered to lie within the physiological to pharmacological concentration range, failed to alter the time course of $I_{Cl(Ca)}$ rundown at +90 mV induced by 3 mM ATP. In contrast, intracellular application of a constitutively active form of PP2A attenuated rundown and led to a potent recovery of late $I_{Cl(Ca)}$ recorded at +90 mV (Fig. 8*B* (*a*)). As expected and similar to the effects of OA (Fig. 4) and cantharidin (Fig. 5), the non-selective PP1/PP2A inhibitor calyculin A (10 nM) blocked the recovery of $I_{Cl(Ca)}$ in 0 ATP and antagonized the action of exogenous PP2A (Fig. 8*B* (*a*)). Because the inclusion of the PP2A inhibitor fostriecin failed to alter $I_{Cl(Ca)}$ in the absence of ATP (Fig. 7), the question of whether this inhibitor was functionally active in our hands became prevalent. To address this concern, we examined the effects of fostricein on the exogenously supplied constitutively active PP2A under conditions that support phosphorylation. The *graph* in Fig. 8*B* (*b*) shows that the addition of 150 nM fostriecin in cells dialyzed with 3 ATP and 200 ng/ml PP2A (*empty circles*) produced a delayed inhibition of the exogenous PP2A-induced stimulation of $I_{Cl(Ca)}$ (*filled squares*) that approached the level reached after 20 min of cell dialysis with 3 mM ATP alone (*empty squares*). These results suggest that the lack of effect of fostriecin on the regulation of $I_{Cl(Ca)}$ by endogenous phosphatases (Fig. 7) cannot be attributed to inefficacy of this compound at inhibiting PP2A. Finally, Fig. 8*C* shows that the response of $I_{Cl(Ca)}$ to exogenous PP2A was also potently inhibited by NIPP-1 (100 pM), which indicates that the apparent regulation of $I_{Cl(Ca)}$ by an excess amount of PP2A in the pipette solution still required PP1 and suggests that the action of PP2A was indirect (see "Discussion").

Are PP1/PP2A and Calcineurin Regulating $I_{Cl(Ca)}$ via a Common Pathway?—Fig. 9*A* (*a*) shows that in cells dialyzed with no ATP, inclusion of a specific peptide inhibitor of CaN (50 μM CaN-AIP) in the pipette solution had a strong inhibitory effect on the recovery of $I_{Cl(Ca)}$, with the peptide exerting an even more potent effect than that reported recently by our group with 10 μM CsA (8). These experiments convincingly show that when the phosphorylation status of the cell is shifted toward phosphatases by omitting ATP, blocking CaN exerts a potent suppression of the recovery of $I_{Cl(Ca)}$.

We also tested the effects of blocking both PP1/PP2A and CaN with 10 nM OA and 50 μM CaN-AIP included in the pipette solution. As illustrated in Fig. 9*A* (*b*), combining the two inhibitors did not lead to more inhibition of the recovery of $I_{Cl(Ca)}$ in the absence of ATP than that produced by a saturating OA concentration alone and was equivalent to that observed with 3 mM ATP in the absence of drug. These results suggest that CaN and PP1/PP2A could be targeting a common signaling pathway, and perhaps one of the two classes of phosphatases may be downstream of the other.

Consistent with our previous study (7), inclusion of CaN Aα in a pipette solution containing 3 mM ATP led to an initial rundown that was followed by recovery of $I_{Cl(Ca)}$, again demonstrating that an exogenous application of calcineurin shifted the phosphorylation balance regulating $I_{Cl(Ca)}$ from kinase to phosphatase (Fig. 9*B*, *empty squares*). Fig. 9*B* shows that inclusion of the PP1-selective blocker, NIPP-1 (100 pM), in the pipette solution strongly inhibited the effects of exogenous CaN Aα (*filled squares*). Taken together, these data suggest that the regulation of $I_{Cl(Ca)}$ by calcineurin and PP1 (and possibly PP2A) appears to be functionally linked through a common pathway.

DISCUSSION

Ca^{2+}-activated Cl^- channels in smooth muscle cells are tightly regulated by one or several phosphorylation mechanisms whose molecular target(s) remain unknown (3–5). The present study further extends this concept by demonstrating for the first time that in addition to Ca^{2+}-calmodulin-regulated calcineurin (7), at least one Ca^{2+}-independent serine/threonine phosphatase (PP1/PP2A) is also involved in regulating native Cl_{Ca} channels. Our study also provides evidence supporting an interaction between CaN Aα and PP1. Our data show that transcripts for several isoforms of these enzymes as well as calcineurin are expressed in the rabbit pulmonary artery. Western blot analysis and immunofluorescence experiments confirmed the presence of several PP1 isoforms and PP2A. In cells dialyzed with no ATP, intracellular application of selective inhibitors of calcineurin or the non-selective PP1/PP2A inhibitors okadaic acid and cantharidin reduced the initial phosphorylation-mediated rundown of $I_{Cl(Ca)}$ and inhibited its delayed recovery. Based on these results, highly selective inhibitors of PP1 and PP2A were used. The PP1 inhibitor NIPP-1 potently inhibited the recovery of $I_{Cl(Ca)}$ in cells dialyzed with no ATP, whereas the PP2A-selective antagonist fostriecin was without effect. In contrast, an exogenous application of PP1 and PP2A yielded different results, with excess PP1 failing to enhance $I_{Cl(Ca)}$ in the pres-

FIGURE 3. **Effects of altering ATP levels and the state of global phosphorylation on Ca^{2+}-activated Cl^- currents elicited by 500 nM Ca^{2+}.** *A*, representative current traces evoked with a 500 nM Ca^{2+} pipette solution containing either no ATP or supplemented with 3 mM ATP. Under conditions supporting global phosphorylation, both the time-dependent outward current at +90 mV and the inward tail current at −80 mV were substantially attenuated over the course of 20 min. However, PA myocytes dialyzed in the absence of exogenous ATP showed enhanced $I_{Cl(Ca)}$, following a transient decline in amplitude, which continued to grow beyond the initial current over the course of the 20-min protocol. Time constants (τ) of activation and deactivation are shown for each representative trace and are displayed for both sets of experiments at $t = 0$, 5, and 20 min. *B*, plot showing the mean time course of changes of normalized late current at +90 mV (1-s steps at 10-s intervals). Currents were normalized against the initial current recorded immediately following membrane rupture ($t = 0$) and plotted as a function of time. Cells dialyzed with 3 mM ATP (*filled squares*; $n = 4$) displayed $I_{Cl(Ca)}$ that declined to ~40% of the initial level after 20 min. $I_{Cl(Ca)}$ recorded from cells dialyzed with a solution lacking ATP (*empty squares*; $n = 7$) ran down to about 75% of its initial amplitude. Recovery of $I_{Cl(Ca)}$ in these cells could be seen as early as 3 min to equal initial amplitude after 15 min and finally exceed it by ~10% after 20 min. ***, significantly different from 3 mM ATP with $p < 0.001$.

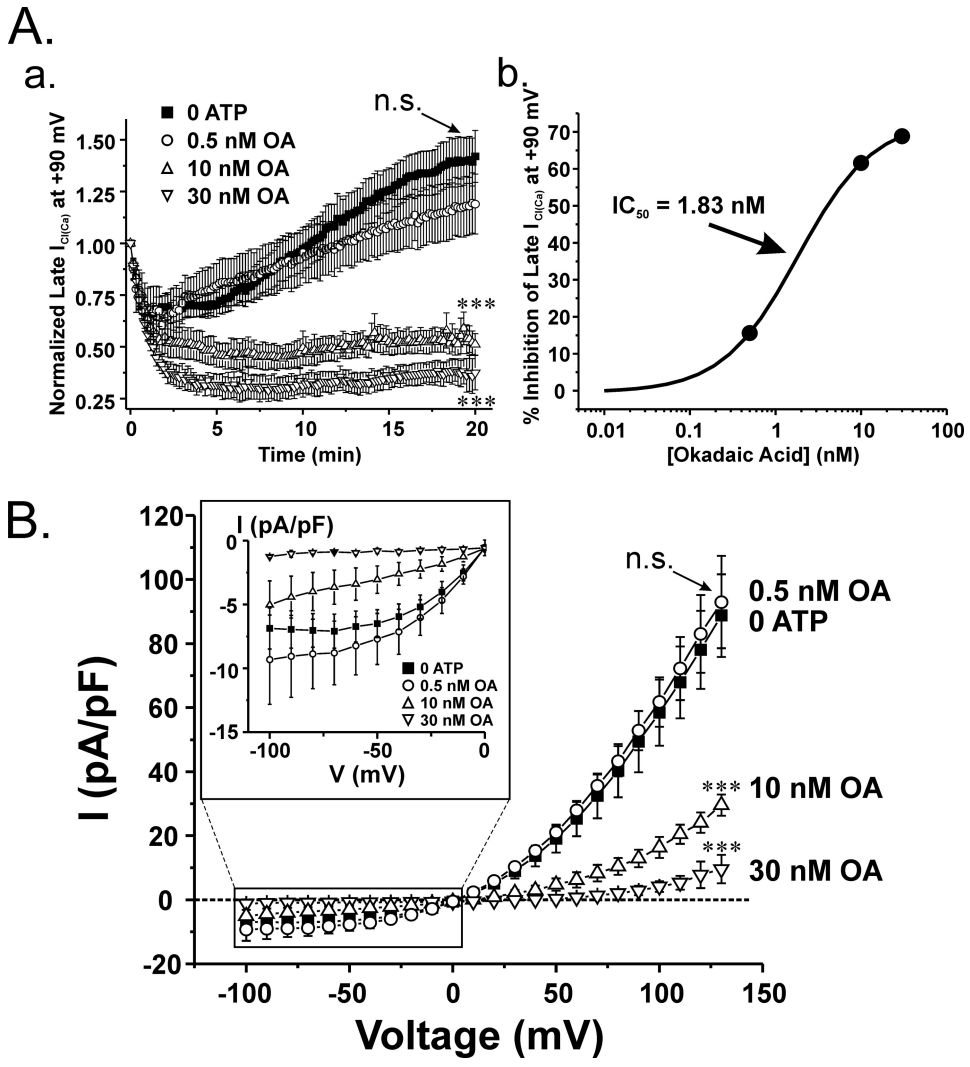

FIGURE 4. **Dose-dependent inhibition of $I_{Cl(Ca)}$ recovery by the non-selective PP1 and PP2A inhibitor okadaic acid.** *A* (*a*), mean time course of changes of normalized $I_{Cl(Ca)}$ for control cells dialyzed with no ATP (*closed squares*; $n = 13$) and cells dialyzed with 0 ATP and 0.5 nM (*open circles*; $n = 5$), 10 nM (*open triangle*; $n = 5$) or 30 nM (*open inverted triangle*; $n = 5$) OA. 0.5 nM OA produced no significant effect on $I_{Cl(Ca)}$ rundown and delayed recovery ($p > 0.05$). Cells dialyzed with 10 or 30 nM OA produced a strong inhibitory effect on Cl_{Ca} channel current recovery, which closely resembles data obtained from cells treated with either CaN inhibitors (Fig. 4) or 3 mM ATP (Fig. 3). One-way ANOVA test at the end of 20 min revealed that the population means were significantly different with $p < 0.001$ (***). Bonferroni *post hoc* tests showed significant differences between 10 and 30 nM and control (no OA; $p < 0.05$), whereas 0.5 nM OA was not significantly different from control ($p > 0.05$). *A* (*b*), dose-dependent curve derived from the data shown in *A* (*a*) after 20 min of cell dialysis with OA. Mean data for the last five traces of normalized late current from our 20-min protocol were used to determine the percentage inhibition using the equation, $((C - OA)/C) \times 100$, where *C* represents control condition, and *OA* indicates myocytes treated with 0.5, 10, or 30 nM OA. Percentage inhibition of late $I_{Cl(Ca)}$ was plotted as a function of OA concentration on a log scale and fitted to a logistic function by nonlinear least-squares fitting provided by Origin version 7.5 to determine the IC_{50}. As shown, the calculated IC_{50} was 1.83 nM. *B*, current-voltage relationships of $I_{Cl(Ca)}$ expressed as current density (pA/picofarads) obtained in the absence or presence of okadaic acid. Higher concentrations of OA (10 and 30 nM) dose-dependently inhibited outwardly rectifying $I_{Cl(Ca)}$, whereas 0.5 nM OA failed to alter $I_{Cl(Ca)}$ magnitude. As for the time courses shown in *A* (*a*), a one-way ANOVA test at +130 mV revealed that the population means were significantly different with $p < 0.001$ (***). Bonferroni *post hoc* tests showed significant differences between 10 and 30 nM and control (no OA; $p < 0.05$), whereas 0.5 nM OA was not significantly different from control ($p > 0.05$). *Inset*, magnified view of the I-V relationships at negative test potentials. *n.s.*, not significant (both *panels*).

ence of 3 mM ATP to support phosphorylation and PP2A causing a delayed stimulation of the current, which could be blocked by fostriecin. Potential mechanisms explaining these results and the functional significance of $I_{Cl(Ca)}$ regulation by Ca^{2+}-dependent and Ca^{2+}-independent phosphatases are discussed below.

Expression of Several Isoforms of Serine/Threonine Phosphatases in Rabbit Pulmonary Artery—We previously reported the unique translocation of CaN Aα from the cytosol to the membrane following elevation of intracellular Ca^{2+} levels. This was paralleled by functional experiments showing that CaN Aα but not CaN Aβ up-regulated $I_{Cl(Ca)}$ in myocytes supplied with 3 mM ATP (7). The present study provided evidence for the expression of mRNA transcripts for both these CaN isoforms, whereas CaN Aγ was undetectable.

Three catalytic isoforms of PP1 ($PP1_c$-α, -β/δ, and -γ) were identified at the mRNA and protein levels. The expressed proteins displayed a molecular mass that is well within the range expected for these isoforms (35–37 kDa) (13). To our knowledge, our study is the first to report the existence of the $PP1_c$-α in smooth muscle cells. In smooth muscle, $PP1_c$-β/δ, commonly referred to as myosin light chain phosphatase, is the major phosphatase controlling the state of phosphorylation of regulatory light chain (LC_{20}) of myosin and muscle relaxation (22, 23). It is therefore not surprising to have detected this isoform in our preparation. $PP1_c$-γ was by far the easiest isoform to detect by reverse transcription-PCR, Western blot, and immunofluorescence. Two splice variants of $PP1_c$-γ, $\gamma 1$ and $\gamma 2$, are expressed in mammalian cells (13, 22). The measured molecular mass of 35 kDa is consistent with $PP1_c$-$\gamma 1$ because $PP1_c$-$\gamma 2$ exhibits a slightly higher molecular mass (39 kDa) (24). $PP1_c$-$\gamma 1$ was recently shown to be expressed in a mouse aortic smooth muscle cell line (25). Finally, two transcripts encoding for the α and β catalytic isoforms of PP2A were detected by reverse transcription-PCR; a PP2A antibody also identified a 36 kDa band consistent with PP2A in many cell types (14), including tracheal smooth muscle (26). Our data thus confirm that the functional significance of Cl_{Ca} channel regulation by both Ca^{2+}-dependent and Ca^{2+}-insensitive serine/threonine phosphatases reported in our study is corroborated by the molecular detection of the key enzymes of interest.

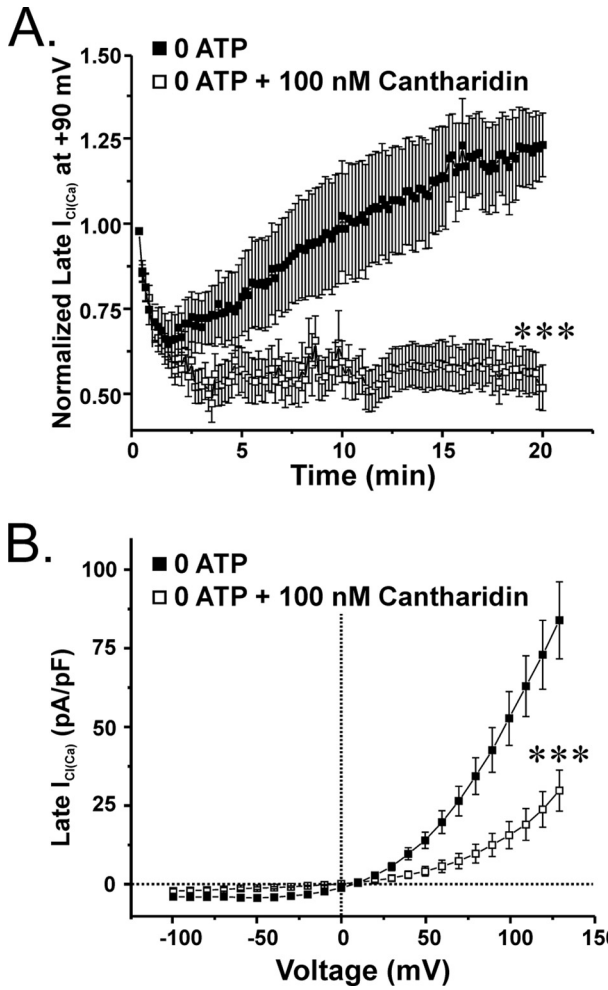

FIGURE 5. **The PP1/PP2A inhibitor cantharidin inhibits the delayed recovery of $I_{Cl(Ca)}$ in pulmonary arterial myocytes dialyzed with no ATP.** *A*, *graph* showing the impact of the internal application of 100 nM cantharidin, a compound displaying higher selectivity for inhibiting PP2A over PP1, on the mean time course of normalized late $I_{Cl(Ca)}$ at +90 mV (1-s steps at 10-s intervals) in cells lacking a supply of exogenous ATP. Cantharidin (*empty squares*; $n = 12$) enhanced the initial rundown of $I_{Cl(Ca)}$ and prevented the delayed recovery seen under control conditions (*filled squares*; $n = 9$). ***, significantly different from control (no cantharidin) with $p < 0.001$. *B*, *graph* showing the mean current-voltage relationships obtained in the presence (*empty squares*; $n = 12$) or absence (*filled squares*; $n = 9$) of 100 nM cantharidin. The inhibitor successfully blocked the outwardly rectifying current by ~58 and 64% at +20 and +130 mV, respectively. At +130 mV, the population means are significantly different with $p < 0.001$ (***). Both control- and cantharidin-treated cells reversed near E_{Cl}.

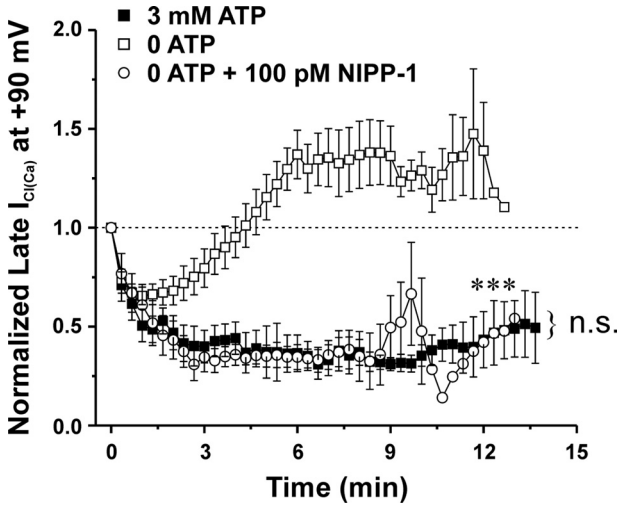

FIGURE 6. **The highly specific endogenous PP1 inhibitor NIPP-1 obliterates the recovery of $I_{Cl(Ca)}$ in the absence of internal ATP.** A *graph* illustrates the mean time course of changes of normalized late $I_{Cl(Ca)}$ recorded at +90 mV (1-s steps at 20-s intervals) in cells dialyzed with 3 mM ATP (*filled squares*; $n = 4$) or in the absence of ATP with (*empty circles*; $n = 5$) or without 100 pM NIPP-1 (*empty squares*; $n = 9$), as indicated. NIPP-1 enhanced $I_{Cl(Ca)}$ rundown and abolished its delayed recovery seen in the absence of ATP (***, $p < 0.001$ relative to 0 ATP and no blockers). The extent of inhibition of $I_{Cl(Ca)}$ by NIPP-1 was similar to the level of rundown induced by 3 mM ATP. *n.s.*, not significant.

Regulation of $I_{Cl(Ca)}$ by Endogenous Serine Threonine Phosphatases—A wide range of non-selective and highly selective inhibitors of protein phosphatases were used in this study and established unequivocally that $I_{Cl(Ca)}$ is regulated by CaN and PP1/PP2A, but for reasons explained below, we speculate that PP1 may be the enzyme regulating these channels. A previous study from our group showed that in cells dialyzed with ATP, the response of $I_{Cl(Ca)}$ to the CaN inhibitor CsA was found to be variable, with one group of cells displaying sensitivity and the other failing to respond to this agent (7). We attributed this observation to a dominance of kinase activity, primarily CaMKII (4), over phosphatase activity, in the control of $I_{Cl(Ca)}$ under a sustained elevation of intracellular $[Ca^{2+}]$. Indeed, $I_{Cl(Ca)}$ entrained by cyclical elevations of $[Ca^{2+}]_i$ due to the opening of voltage-gated Ca^{2+} channels was consistently inhibited by CsA, a situation that would be expected to yield a lower state of CaMKII autophosphorylation and thus a higher contribution from phosphatases (7). In this particular study, we showed that when the influence of kinases was blunted by lack of substrate, blocking CaN with the specific autoinhibitory peptide (CaN-AIP) led to enhancement of the initial rundown of $I_{Cl(Ca)}$ and suppression of its delayed recovery. Our interpretation of these results is that at the time of rupturing the seal, endogenous ATP levels are utilized by kinases to phosphorylate the channel or a regulatory subunit in the channel complex, which leads to $I_{Cl(Ca)}$ inactivation (6). As cellular ATP levels get depleted over time, phosphatases take over and promote Cl_{Ca} channel recovery, a process that can be blocked by inhibiting CaN with CaN-AIP (this study) or CsA (8).

The widely used PP1/PP2A inhibitor okadaic acid dose-dependently enhanced the rundown of $I_{Cl(Ca)}$ and inhibited its delayed recovery in PA myocytes dialyzed with no ATP to promote dephosphorylation by endogenous phosphatases. After 20 min, the IC_{50} of OA for blocking recovery of late current elicited at +90 mV was ~2 nM, and a maximal effect requiring more than 30 nM was comparable with that achieved by CaN inhibitors. At any of the concentrations tested, OA has no effect on protein kinase A, protein kinase C, and CaMKII activities (16, 27). Possible complicating effects of kinases were minimized by removing ATP from the pipette solution, which probably severely depleted endogenous stores of the nucleotide, leaving little substrate for phosphorylation. Although it is not possible to conclude in favor of either enzyme, the measured IC_{50} of 2 nM OA and estimated concentration required (>30–50 nM) to yield a maximal response (IC_{50} for blocking PP2A, 0.01–1 nM; IC_{50} for blocking PP1, 3–100 nM) (15–20, 27, 28) would be more consistent with PP1. Another non-selective

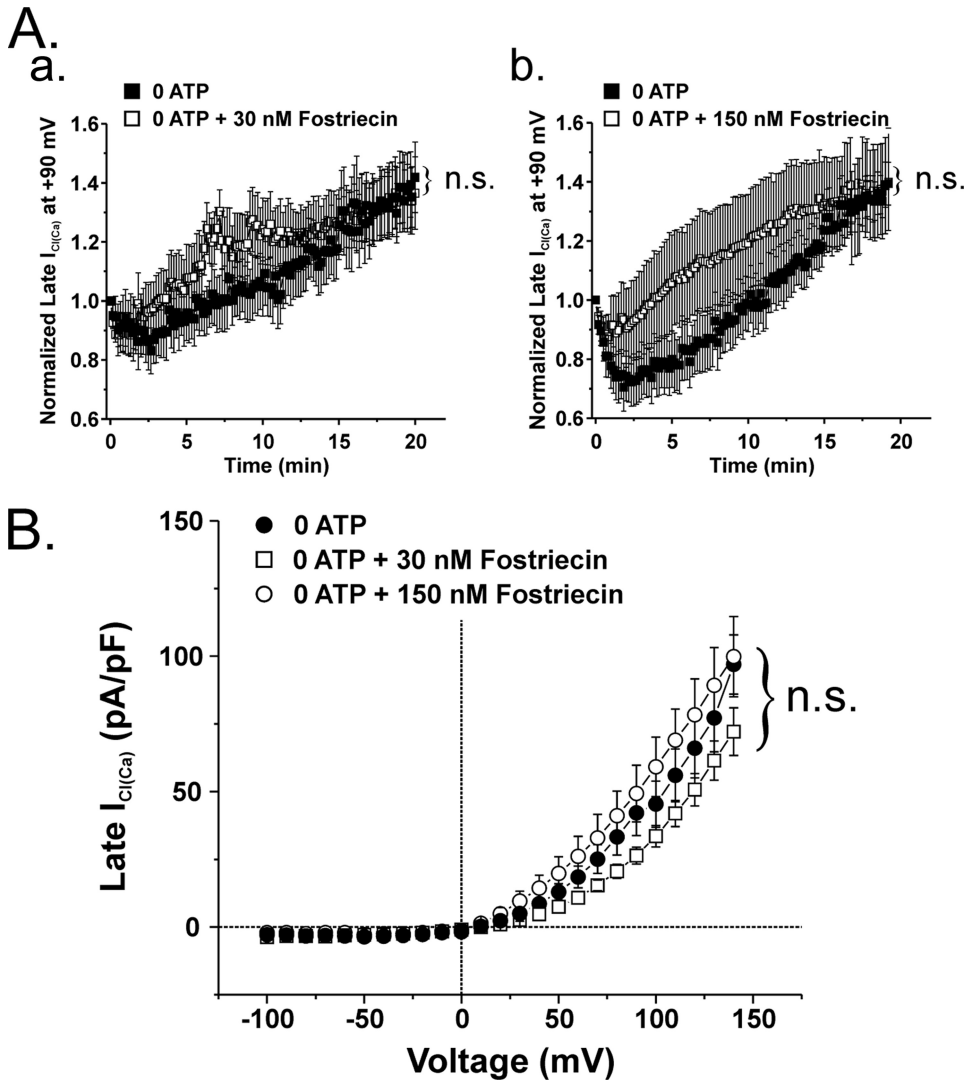

FIGURE 7. **The highly selective inhibitor of PP2A fostriecin has no effect on $I_{Cl(Ca)}$ recorded in the absence of internal ATP.** *A* (*a*), plot showing the time course of changes of mean normalized late $I_{Cl(Ca)}$ recorded at +90 mV (1-s steps at 10-s intervals) in cells dialyzed with no ATP, in the presence (*empty squares*; $n = 10$) or absence (*filled squares*; $n = 7$) of 30 nM fostriecin, a concentration ~10-fold higher than the IC_{50} for PP2A (3.2 nM). At this concentration, the compound failed to alter $I_{Cl(Ca)}$ amplitude at +90 mV during the initial rundown and late recovery over the course of 20 min. *A* (*b*), similar *graph* to that shown in *A* (*a*) except that for these experiments, fostriecin concentration was raised to 150 nM (47-fold higher than the IC_{50} for PP2A). Data obtained with (*empty squares*) or without (*filled squares*) fostriecin were obtained from 7 and 10 cells, respectively. Similar to the results illustrated previously, this concentration of fostriecin was unsuccessful in attenuating the recovery of late $I_{Cl(Ca)}$. *B*, current-voltage relationships for late $I_{Cl(Ca)}$ in cells dialyzed with 0 ATP, in the absence (*filled squares*; $n = 3$) or presence of 30 (*empty squares*; $n = 3$) or 150 nM (*empty circles*; $n = 2$) fostriecin. All I-V values were obtained immediately following the conclusion of the 20-min test protocol. Consistent with the data presented in *A*, this *graph* illustrates the lack of effect of fostriecin on $I_{Cl(Ca)}$ at voltages ranging from −100 to +130 mV. *n.s.*, not significant (all *panels*).

but less potent PP1/PP2A inhibitor than OA, cantharidin, also blocked the recovery of $I_{Cl(Ca)}$. As for OA, cantharidin offers some selectivity for preferentially blocking PP2A over PP1, although the range is quite narrow with a ~10-fold difference in IC_{50} values. The reported IC_{50} ranges for blocking PP2A and PP1 are 40–200 and 473–2000 nM, respectively (17, 19). In contrast to OA, at the concentration used in our study (100 nM), cantharidin would be expected to preferentially block PP2A. However, we have to be careful before making conclusions about the identity of the phosphatase involved based on the above results because the extracted values were obtained from enzyme assays carried out under very specific conditions (different substrates, cell lysates, or homogenate extracts, etc.). As an example, Obara and Yabu (29) showed that L-type Ca^{2+} current (I_{CaL}) in guinea pig intestinal smooth muscle cells is dually regulated by protein phosphatases. At low concentrations, OA dose-dependently inhibited I_{CaL}, with maximal inhibition occurring at 10 nM. At concentrations of >100 nM, OA increased I_{CaL}, with a maximal effect seen at ~1 μM. These inhibitory and stimulatory responses were ascribed to reflect dephosphorylation of two distinct targets by PP2A and PP1, respectively. In another study, OA was shown to stimulate unitary Ca^{2+} channel activity in human vascular smooth muscle cells, and 1 μM OA was necessary to achieve maximal effect (30). The involvement of PP2A but not PP1 was directly assessed by testing the effects of OA on single Ca^{2+} channels exposed to $PP2A_c$ or $PP1_c$ from the internal side of inside-out patches. The functional effects of OA in intact cells were thus observed at concentrations that are significantly higher than those required for blocking either enzyme in biochemical assays.

Experiments were subsequently undertaken to consolidate the view that PP1 drives Cl^- channel recovery. Fostriecin is an antitumor antibiotic agent isolated from the fermentation beer of *Saccharomyces pulveraceus* (20). This compound is ~40,000-fold more effective at inhibiting PP2A (IC_{50} = 3.2 nM) over PP1 (IC_{50} = 131 μM), and has no influence on CaN. Inclusion of fostriecin at a concentration either ~9- or 47-fold above its IC_{50} for blocking PP2A failed to alter the time course of $I_{Cl(Ca)}$ rundown and delayed recovery. We were careful in preparing a fresh stock daily, and significant inhibitory activity was never encountered when testing a new sample prepared from a sealed vial. Moreover, 150 nM fostriecin effectively inhibited the stimulatory response on $I_{Cl(Ca)}$ mediated by exogenous PP2A (see below), strongly suggesting that its lack of effect in cells dialyzed with no ATP was not due to its inefficacy.

In contrast to fostriecin, dialysis with only a 100 pM concentration of the highly specific and endogenous inhibitor of PP1, NIPP-1 (IC_{50} < 1 pM) (19), obliterated the recovery of $I_{Cl(Ca)}$. This polypeptide is a natural targeting regulator of PP1 that

associates with RNA and plays an important role in processing pre-mRNA and splicing (22). The association of NIPP-1 with PP1 is highly regulated by at least one phosphorylation step (31, 32). The above results with phosphatase-selective inhibitors would suggest that endogenous PP1 rather than PP2A regulates Cl_{Ca} channels in our conditions. The molecular identity of Cl_{Ca} channels in vascular smooth muscle cells is still unknown. Two families of Cl^- channel genes, the bestrophins (*BEST1* to *-4* in

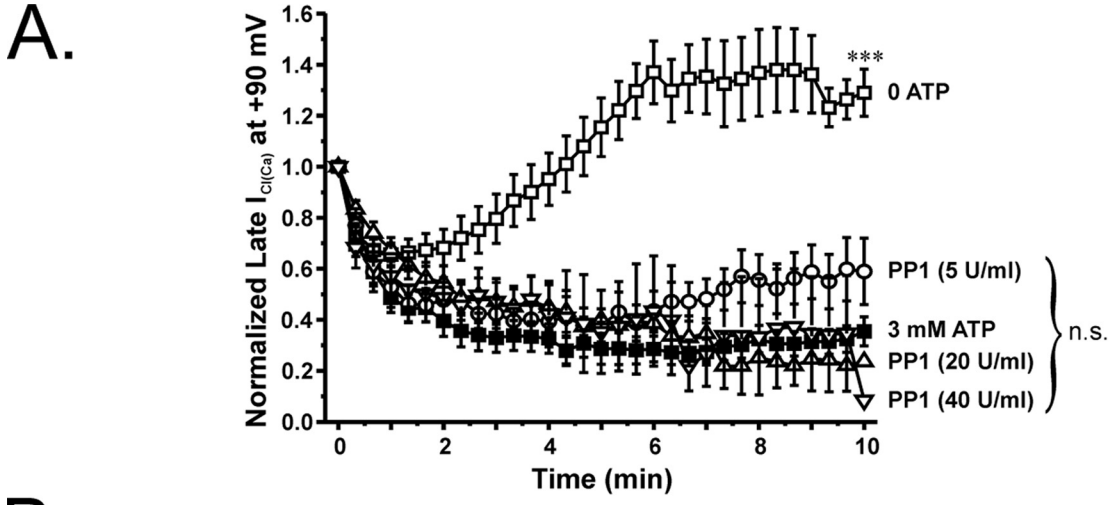

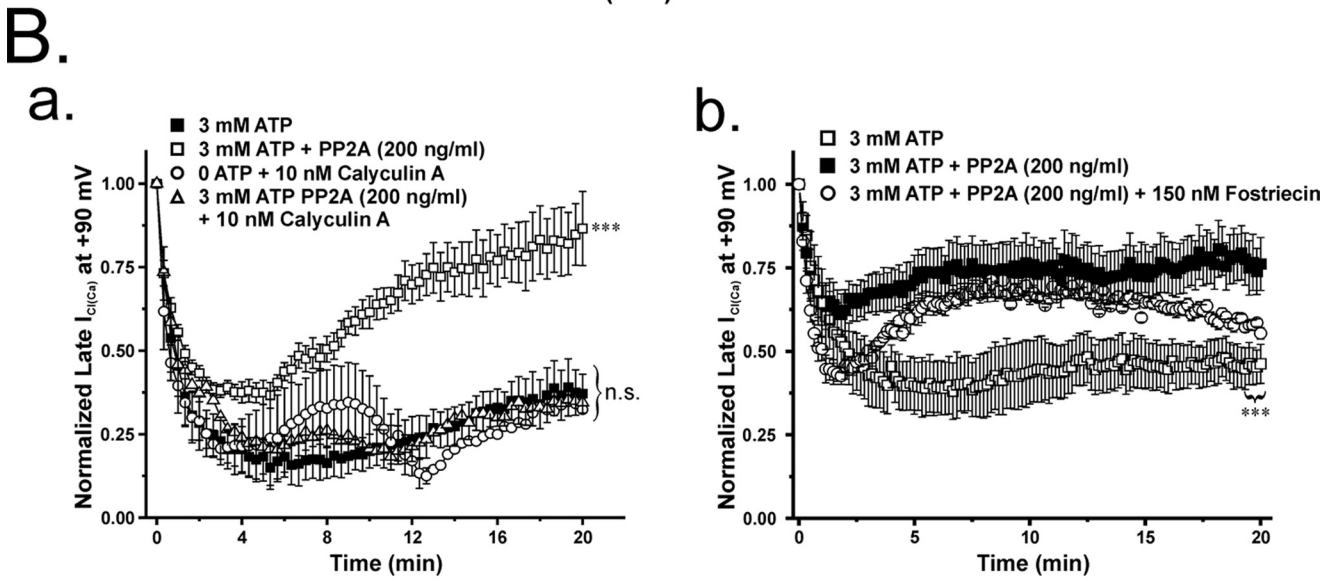

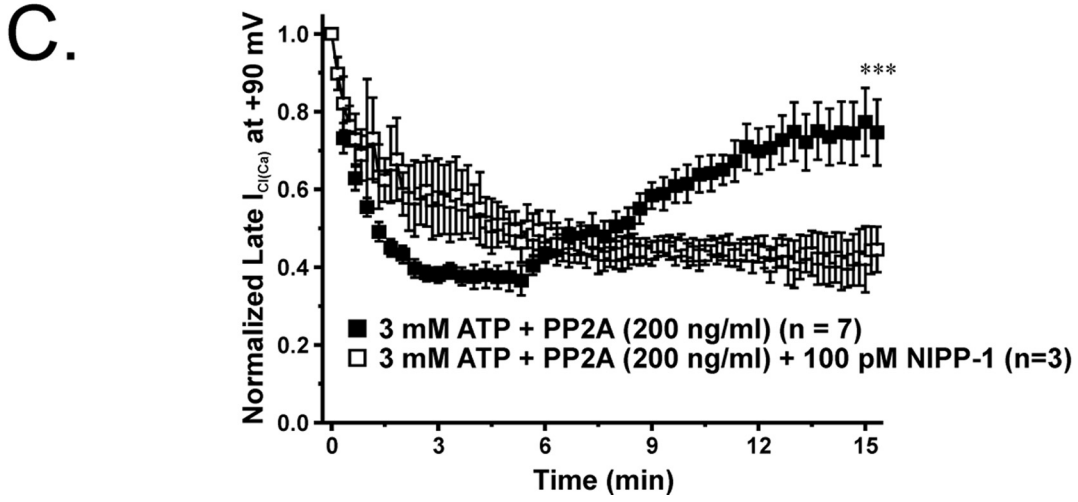

humans) and *TMEM16A/B* (anoctamin; 2 of 10 paralogs), have recently emerged as candidate gene families for Cl_{Ca} channels (3, 33–36), but *TMEM16A/B* genes appear as more promising candidates because their biophysical properties are more similar to the native smooth muscle channel when expressed in heterologous expression systems (34–36). Both classes of Cl_{Ca} channel genes exhibit several consensus sequences for phosphorylation by serine/threonine protein kinases, including CaMKII. Future site-directed mutagenesis experiments are planned to determine the potential role of these sites in regulating Cl_{Ca} channels. Interestingly, BEST1 (bestrophin isoform 1 or vitelliform macular dystrophy type 2 gene), one of four human genes, is expressed in the rabbit pulmonary artery (3) and was demonstrated to be dephosphorylated by PP2A via a direct physical interaction (37). If BEST1 turns out to be a contributor to the pore-forming subunit of the Cl_{Ca} channel, it will be important to determine if PP2A is physically associated and functionally interacts with BEST1 in a manner consistent with our data on regulation of the native Cl_{Ca} channel.

Response of $I_{Cl(Ca)}$ to Exogenous Catalytic Subunits of PP1 and PP2A—Cell dialysis with purified catalytic subunits of PP1 and PP2A resulted in opposite and unsuspected effects on $I_{Cl(Ca)}$. In these experiments, the cells were dialyzed with 3 mM ATP to support phosphorylation, and excess amounts of $PP1_c$ or $PP2A_c$ were added to the pipette solution. This strategy was used previously to successfully demonstrate that CaN Aα but not CaN Aβ can up-regulate $I_{Cl(Ca)}$ in rabbit PA myocytes (7). At a concentration (5 units/ml) proven to modulate cystic fibrosis transmembrane regulator Cl^- channels in 3T3 fibroblasts and CHO cells (38, 39) $PP1_c$ was without effect. Increasing the concentration of the phosphatase up to 8-fold failed to revert the rundown of $I_{Cl(Ca)}$. On the contrary, inclusion of $PP2A_c$ in the pipette solution led to progressive recovery of $I_{Cl(Ca)}$. Without results from many more experiments, we can only speculate on possible mechanisms. Both types of enzyme are holoenzymes composed of scaffolding, interacting, and catalytic subunits, and recent studies have provided convincing evidence that the exact composition of the many possible holoenzymes is responsible for their subcellular distribution and regulation in specific organelles and that it confers substrate preferences (13, 14, 22). It is possible that exogenously added $PP1_c$ cannot reach its final target due to steric hindrance or is unable to assemble with the holoenzyme counterparts that are necessary to induce the dephosphorylation step regulating Cl_{Ca} channels. Another possibility is that the endogenous phosphatase may be so tightly associated with the channel via chaperone and anchoring proteins that it cannot be displaced by excess exogenous protein. In contrast, PP2A may be able to reach the target site and in excess amounts able to compete and overwhelm CaMKII. Perhaps a more attractive hypothesis to explain the effects of $PP2A_c$ is that exogenously added enzyme inactivates constitutively active CaMKII, an excellent substrate for PP2A (28, 40), which would in turn shift the phosphorylation potential balance toward the endogenous phosphatases. This possibility is supported by the observation that the fostriecin-sensitive response of $I_{Cl(Ca)}$ to PP2A was also potently inhibited by NIPP-1. The physiological significance of supplying excess amounts of enzyme must be interpreted with caution because almost any phosphorylated protein may be ultimately dephosphorylated by a physiologically irrelevant phosphatase if a sufficient amount is supplied.

Physiological Significance of Cl_{Ca} Channel by CaN and PP1/PP2A—One very intriguing observation from our data is that either CaN or PP1/PP2A is capable of regulating Cl_{Ca} channels fully, indicating that the effects of both classes of phosphatases are not superimposed. In other words, when blocking either type of enzyme, the other class is unable to compensate. This suggests that CaN and PP1/PP2A are somehow linked directly or indirectly in regulating the Cl_{Ca} channel. One possibility is that there are two distinct phosphorylation sites regulating the channel, each targeted by one class of phosphatases, and both phosphate groups have to be removed for the channel to recover from phosphorylation-induced block. An alternative and more attractive hypothesis is the possibility that the two phosphatases act in concert, with one regulated by the other in a downstream pathway involving phosphorylation. Such a cascade involving CaN and PP1 has been reported to play a role in long term depression and memory in the hippocampus (41). In this tissue, Ca^{2+} entry through *N*-methyl-D-aspartate receptors binds to calmodulin and stimulates CaN, which then dephosphorylates a high affinity PP1 inhibitor called I-1 (inhibitor of protein phosphatase type 1). When

FIGURE 8. **Effects of internal application of a constitutively active form of PP1 or PP2A on phosphorylation-induced rundown of $I_{Cl(Ca)}$.** To further elucidate the role of Ca^{2+}-independent phosphatases, we investigated the effects of supplying constitutively an active form of PP1 or PP2A intracellularly. In these experiments, the pipette solution contained 3 mM ATP to support phosphorylation. *A*, *graph* showing the mean time course of changes of normalized late $I_{Cl(Ca)}$ recorded at +90 mV (1-s steps applied at 20-s intervals) in the presence of ATP only (*filled squares*; $n = 10$) or with 3 mM ATP and one of three PP1 concentrations ranging from 5 to 40 units/ml, as indicated ($n = 7–8$ per group of cells). All three PP1 concentrations failed to significantly influence the time course of $I_{Cl(Ca)}$ rundown induced by 3 mM ATP. A one-way ANOVA test revealed that the population means were significantly different with $p < 0.001$ (***). Bonferroni *post hoc* tests showed significant differences between all conditions, including drugs and 3 mM ATP, and 0 ATP ($p < 0.05$); no significant differences were noted between ATP alone and ATP plus any of the three PP1 concentrations tested ($p > 0.05$). *B* (*a*) *graph* similar to that displayed in *A* showing the effect of intracellular application of PP2A (200 ng/ml; *empty squares*; $n = 5$) on the mean time course of normalized late $I_{Cl(Ca)}$ recorded at +90 mV (1-s steps applied at 20-s intervals). PP2A successfully reserved the rundown of $I_{Cl(Ca)}$ induced by 3 mM ATP (*filled squares*; $n = 4$). The cells concurrently treated with PP2A and calyculin A (10 nM), a potent inhibitor of PP1/PP2A, reversed the recovery of late $I_{Cl(Ca)}$ seen with PP2A alone (empty circles; $n = 5$). A one-way ANOVA test revealed that the population means were significantly different with $p < 0.001$ (***). Bonferroni *post hoc* tests showed significant differences between PP2A and 3 mM ATP and all other groups; all other comparisons were not significant ($p > 0.05$). Similar to OA, cantharidin, and NIPP-1, intracellular application of calyculin A alone suppressed the recovery of $I_{Cl(Ca)}$ in cells dialyzed with no ATP (*empty triangles*; $n = 2$). *n.s.*, not significant (both *panels*). *B* (*b*), *graph* displaying the mean time course of normalized late $I_{Cl(Ca)}$ at +90 mV in the presence of ATP only (*open squares*; $n = 4$) or accompanied with either PP2A (200 ng/ml; *filled squares*; $n = 8$) or PP2A and fostriecin (150 nM; *open circles*; $n = 2$). A one-way ANOVA test revealed that the population means were significantly different with $p < 0.001$ (***). Bonferroni *post hoc* tests showed significant differences between 3 mM ATP, PP2A, and PP2A plus fostriecin. *C*, *graph* illustrating the mean time course of normalized late $I_{Cl(Ca)}$ at +90 mV in the presence of either 3 mM ATP and PP2A (200 ng/ml) (*filled squares*) or 3 mM ATP, PP2A, and 100 pM NIPP-1 (*empty squares*). Unpaired student *t* test exhibited statistical significant differences with $p < 0.001$ (***) between cells dialyzed with 3 mM ATP + PP2A and those cells presented with 3 mM ATP + PP2A + NIPP-1.

phosphorylated, I-1 is tightly bound to PP1 and inhibits it. CaN-mediated dephosphorylation of I-1 thus activates PP1. I-1 (as well as an isoform of I-1 called DARPP-32 (dopamine- and cyclic AMP-regulated phosphoprotein with molecular mass of 32 kDa)) is phosphorylated by protein kinase A when the neurotransmitter dopamine activates D1-type receptors in the brain (22, 42). This mechanism operates in many cell types where Ca^{2+} and cAMP have antagonistic effects, which is the

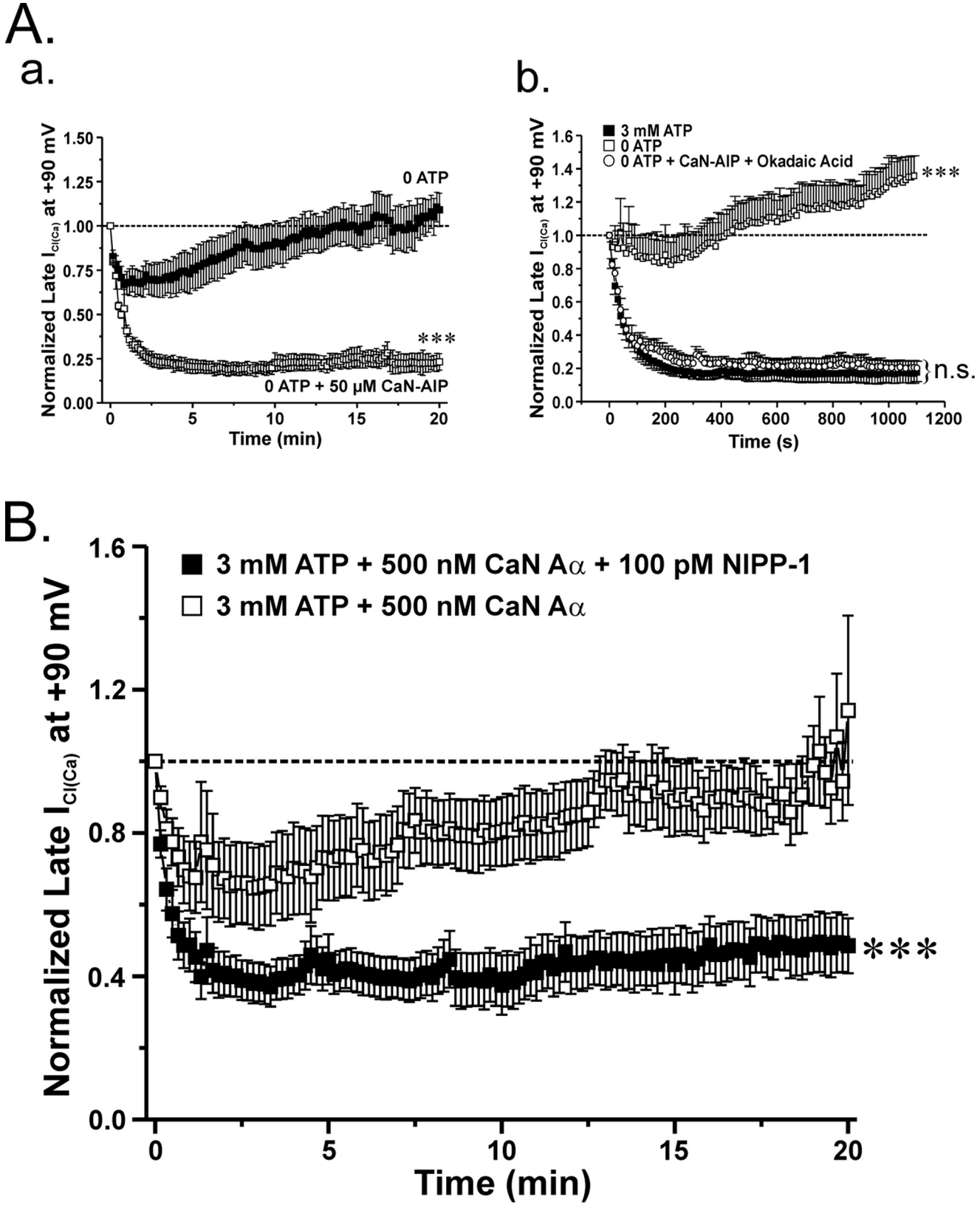

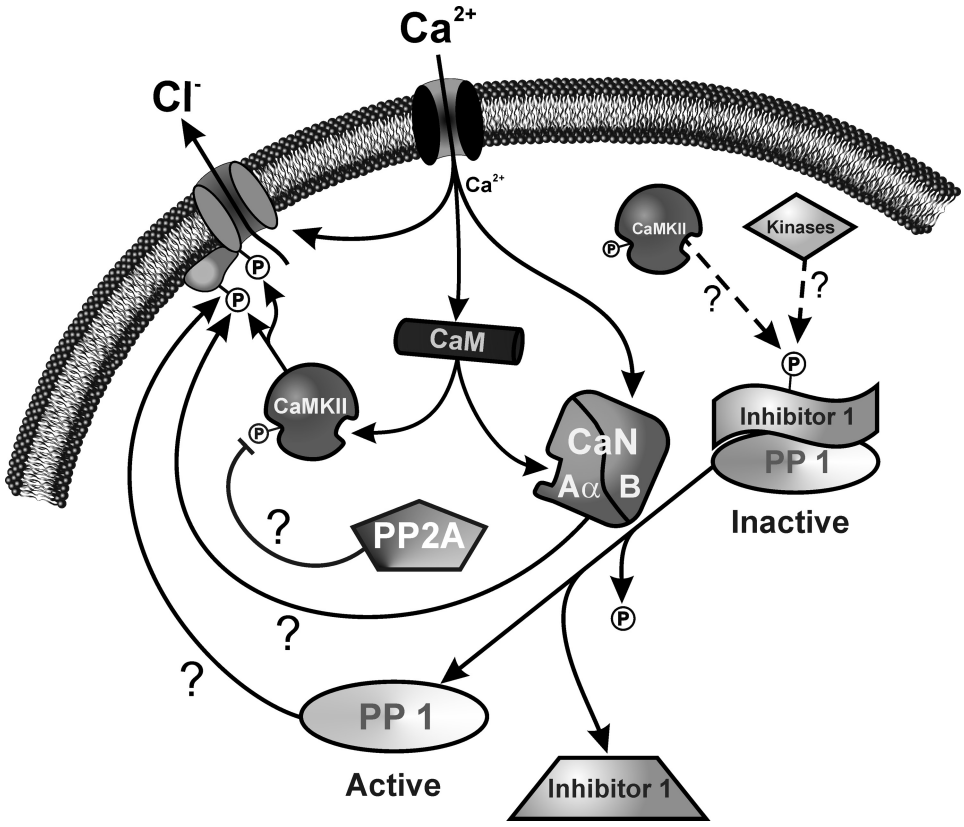

FIGURE 10. **Proposed schematic representation of Cl_{Ca} channel regulation by CaMKII and Ca^{2+}-dependent and -independent phosphatases in pulmonary arterial smooth muscle cells.** As intracellular Ca^{2+} levels rise in pulmonary artery smooth muscle cells, Cl_{Ca} channels are directly activated by Ca^{2+} and modulated by phosphorylation involving CaMKII and CaN Aα via Ca^{2+} binding to Ca^{2+}-calmodulin and calcineurin B (*CaN B*). In the presence of ATP, CaMKII phosphorylation is favored over the effects produced by phosphatases. In the absence of ATP, this balance is shifted toward phosphatases, yielding up-regulation of $I_{Cl(Ca)}$ following a transient state of phosphorylation due to consumption of the endogenous substrate. Under these conditions, dephosphorylation of I-1 by CaN Aα would relieve its inhibitory effect on PP1, which would then dephosphorylate the pore-forming or accessory subunit.

case in vascular smooth muscle cells (43). When $[Ca^{2+}]_i$ rises, relief of the inhibitory effect of I-1 on PP1 by CaN also causes dephosphorylation of CaMKII, at least *in vitro*, which would also promote dephosphorylation of the Cl_{Ca} channel. The possibility that this pathway also exists in pulmonary artery smooth muscle cells is supported by the observation that the enhancement of $I_{Cl(Ca)}$ by CaN Aα (this study) (7) was potently inhibited by NIPP-1. There is little evidence for regulation of CaN by phosphorylation (42, 44, 45), which supports the idea that CaN would be acting upstream of PP1. Fig. 10 shows a *schematic diagram* illustrating our working model and the hypothetical steps believed to regulate Cl_{Ca} channels. In this model, PP1 is the ultimate phosphatase dephosphorylating the channel or a regulatory subunit. When intracellular Ca^{2+} levels rise, this activates Cl_{Ca} channels directly, and both CaMKII and CaN Aα via binding of Ca^{2+}-calmodulin. In the presence of ATP, for reasons that are still unclear, the impact of CaMKII phosphorylation is greater than that produced by phosphatases (7). In the absence of ATP, this balance is shifted toward phosphatases, yielding up-regulation of $I_{Cl(Ca)}$ following a transient state of phosphorylation due to consumption of endogenous ATP. Under these conditions, dephosphorylation of I-1 by CaN Aα would relieve its inhibitory effect on PP1, which would then dephosphorylate the pore-forming subunit or accessory subunit. The goal of future experiments will be to assess the potential role of I-1 in this signaling pathway and identify the kinase (protein kinase A, CaMKII, or others?) phosphorylating this regulator.

Conclusion—The results presented herein demonstrate that the regulation of excitatory Cl_{Ca} channels by kinases and phosphatases in pulmonary arterial smooth muscle cell is significantly more complicated than previously anticipated. Cl_{Ca} channels are regulated by at least one kinase, CaMKII, which serves as a braking mechanism to offset the depolarizing influence of Cl_{Ca} channels during signaling (3, 4, 6). This CaMKII-induced phosphorylation is antagonized by a Ca^{2+}-dependent mechanism, involving CaN Aα, and for the first time a Ca^{2+}-independent step mediated probably by PP1 but also maybe PP2A. Our data convincingly show that both classes of enzymes are absolutely necessary to oppose kinase activity and stimulate Cl_{Ca} channels. Future experiments will be conducted to define the molecular steps involved in the interplay between CaMKII, CaN, and PP1/PP2A in the regulation of Ca^{2+}-activated Cl^- conductance of the pulmonary arterial vasculature.

FIGURE 9. **A functional link between calcineurin and PP1 appears to exist when it comes to the regulation of $I_{Cl(Ca)}$ in rabbit pulmonary artery smooth muscle cells.** *A* (*a*), mean time course of changes of normalized $I_{Cl(Ca)}$ amplitude in the presence (*open squares*; $n = 4$) or absence (*closed squares*; $n = 5$) of 50 μM calcineurin autoinhibitory peptide (CaN-AIP). Exposure to 50 μM CaN-AIP suppressed the recovery of $I_{Cl(Ca)}$. Cl_{Ca} currents were reduced by ~80% after 20 min when compared with control conditions. ***, significantly different from control (no CaN-AIP) with $p < 0.001$. *A* (*b*), *graph* showing the mean time course of changes of normalized $I_{Cl(Ca)}$ at +90 mV (1-s steps at 10-s intervals) in cells dialyzed with 3 mM ATP (*filled squares*; $n = 5$) or no ATP, with (*empty circles*; $n = 4$) or without (*empty squares*; $n = 5$) 10 nM OA (PP1/PP2A inhibitor) and 50 μM CaN-AIP (CaN inhibitor). A one-way ANOVA test at the end of 20 min revealed that the population means were significantly different with $p < 0.001$ (***). *n.s.*, not significant. *B*, to determine whether a functional link exists between CaN and PP1, our group examined the effects of the constitutively active calcineurin isoform CaN Aα in the presence of the PP1-specific inhibitor NIPP-1 under conditions that support phosphorylation. As indicated by the *graph*, which represents normalized late $I_{Cl(Ca)}$ at +90 mV plotted as a function of time, 500 nM CaN Aα fully reverses the phosphorylation-mediated rundown of $I_{Cl(Ca)}$ (*open squares*; $n = 7$). On the contrary, the effect of CaN Aα on $I_{Cl(Ca)}$ recovery was significantly attenuated with the addition of 100 pM NIPP-1 to the pipette solution (*closed squares*; $n = 10$). The degree of rundown produced by 100 pM NIPP-1 was similar to that seen with 3 mM ATP. ***, significantly different from 3 mM ATP + 500 nM CaN Aα with $p < 0.001$.

Acknowledgments—We thank Catherine Lachendro, Janice Tinney, and Marissa Huebner for technical support in isolating pulmonary artery smooth muscle cells and preparing solutions.

REFERENCES

1. Chipperfield, A. R., and Harper, A. A. (2000) *Prog. Biophys. Mol. Biol.* **74,** 175–221
2. Large, W. A., and Wang, Q. (1996) *Am. J. Physiol.* **271,** C435–C454
3. Leblanc, N., Ledoux, J., Saleh, S., Sanguinetti, A., Angermann, J., O'Driscoll, K., Britton, F., Perrino, B. A., and Greenwood, I. A. (2005) *Can J. Physiol. Pharmacol.* **83,** 541–556
4. Greenwood, I. A., Ledoux, J., and Leblanc, N. (2001) *J. Physiol.* **534,** 395–408
5. Wang, Y. X., and Kotlikoff, M. I. (1997) *Proc. Natl. Acad. Sci. U.S.A.* **94,** 14918–14923
6. Angermann, J. E., Sanguinetti, A. R., Kenyon, J. L., Leblanc, N., and Greenwood, I. A. (2006) *J. Gen. Physiol.* **128,** 73–87
7. Greenwood, I. A., Ledoux, J., Sanguinetti, A., Perrino, B. A., and Leblanc, N. (2004) *J. Biol. Chem.* **279,** 38830–38837
8. Wiwchar, M., Ayon, R., Greenwood, I. A., and Leblanc, N. (2009) *Br. J. Pharmacol.*, in press
9. Ledoux, J., Greenwood, I., Villeneuve, L. R., and Leblanc, N. (2003) *J. Physiol.* **552,** 701–714
10. Perrino, B. A., Fong, Y. L., Brickey, D. A., Saitoh, Y., Ushio, Y., Fukunaga, K., Miyamoto, E., and Soderling, T. R. (1992) *J. Biol. Chem.* **267,** 15965–15969
11. Perrino, B. A., Ng, L. Y., and Soderling, T. R. (1995) *J. Biol. Chem.* **270,** 340–346
12. Perrino, B. A., Wilson, A. J., Ellison, P., and Clapp, L. H. (2002) *Eur. J. Biochem.* **269,** 3540–3548
13. Ceulemans, H., and Bollen, M. (2004) *Physiol. Rev.* **84,** 1–39
14. Janssens, V., Longin, S., and Goris, J. (2008) *Trends Biochem. Sci.* **33,** 113–121
15. Cohen, P., Holmes, C. F., and Tsukitani, Y. (1990) *Trends Biochem. Sci.* **15,** 98–102
16. Haystead, T. A., Sim, A. T., Carling, D., Honnor, R. C., Tsukitani, Y., Cohen, P., and Hardie, D. G. (1989) *Nature* **337,** 78–81
17. Honkanen, R. E. (1993) *FEBS Lett.* **330,** 283–286
18. Ishihara, H., Martin, B. L., Brautigan, D. L., Karaki, H., Ozaki, H., Kato, Y., Fusetani, N., Watabe, S., Hashimoto, K., and Uemura, D. (1989) *Biochem. Biophys. Res. Commun.* **159,** 871–877
19. Sheppeck, J. E., 2nd, Gauss, C. M., and Chamberlin, A. R. (1997) *Bioorg. Med. Chem.* **5,** 1739–1750
20. Walsh, A. H., Cheng, A., and Honkanen, R. E. (1997) *FEBS Lett.* **416,** 230–234
21. Beullens, M., Van Eynde, A., Stalmans, W., and Bollen, M. (1992) *J. Biol. Chem.* **267,** 16538–16544
22. Cohen, P. T. (2002) *J. Cell Sci.* **115,** 241–256
23. Hartshorne, D. J., Ito, M., and Erdödi, F. (2004) *J. Biol. Chem.* **279,** 37211–37214
24. Shima, H., Haneji, T., Hatano, Y., Kasugai, I., Sugimura, T., and Nagao, M. (1993) *Biochem. Biophys. Res. Commun.* **194,** 930–937
25. Tchivilev, I., Madamanchi, N. R., Vendrov, A. E., Niu, X. L., and Runge, M. S. (2008) *J. Biol. Chem.* **283,** 22193–22205
26. Zhou, X. B., Ruth, P., Schlossmann, J., Hofmann, F., and Korth, M. (1996) *J. Biol. Chem.* **271,** 19760–19767
27. Bialojan, C., and Takai, A. (1988) *Biochem. J.* **256,** 283–290
28. Barnes, G. N., Slevin, J. T., and Vanaman, T. C. (1995) *J. Neurochem.* **64,** 340–353
29. Obara, K., and Yabu, H. (1993) *Am. J. Physiol.* **264,** C296–C301
30. Groschner, K., Schuhmann, K., Mieskes, G., Baumgartner, W., and Romanin, C. (1996) *Biochem. J.* **318,** 513–517
31. Beullens, M., Vulsteke, V., Van Eynde, A., Jagiello, I., Stalmans, W., and Bollen, M. (2000) *Biochem. J.* **352,** 651–658
32. Comerford, K. M., Leonard, M. O., Cummins, E. P., Fitzgerald, K. T., Beullens, M., Bollen, M., and Taylor, C. T. (2006) *J. Cell. Physiol.* **209,** 211–218
33. Hartzell, H. C., Qu, Z., Yu, K., Xiao, Q., and Chien, L. T. (2008) *Physiol. Rev.* **88,** 639–672
34. Caputo, A., Caci, E., Ferrera, L., Pedemonte, N., Barsanti, C., Sondo, E., Pfeffer, U., Ravazzolo, R., Zegarra-Moran, O., and Galietta, L. J. (2008) *Science* **322,** 590–594
35. Schroeder, B. C., Cheng, T., Jan, Y. N., and Jan, L. Y. (2008) *Cell* **134,** 1019–1029
36. Yang, Y. D., Cho, H., Koo, J. Y., Tak, M. H., Cho, Y., Shim, W. S., Park, S. P., Lee, J., Lee, B., Kim, B. M., Raouf, R., Shin, Y. K., and Oh, U. (2008) *Nature* **455,** 1210–1215
37. Marmorstein, L. Y., McLaughlin, P. J., Stanton, J. B., Yan, L., Crabb, J. W., and Marmorstein, A. D. (2002) *J. Biol. Chem.* **277,** 30591–30597
38. Berger, H. A., Travis, S. M., and Welsh, M. J. (1993) *J. Biol. Chem.* **268,** 2037–2047
39. Luo, J. X., Pato, M. D., Riordan, J. R., and Hanrahan, J. W. (1998) *Am. J. Physiol. Cell Physiol.* **43,** C1397–C1410
40. Strack, S., Barban, M. A., Wadzinski, B. E., and Colbran, R. J. (1997) *J. Neurochem.* **68,** 2119–2128
41. Mulkey, R. M., Endo, S., Shenolikar, S., and Malenka, R. C. (1994) *Nature* **369,** 486–488
42. Perrino, B. A., Soderling, S. R., Van Eldik, L., and Watterson, D. M. (1998) in *Biochemistry and Pharmacology of Calmodulin-regulated Phosphatase Calcineurin*, pp. 169–236, Academic Press, Inc., Toronto
43. McDaniel, N. L., Rembold, C. M., and Murphy, R. A. (1994) *Can. J. Physiol. Pharmacol.* **72,** 1380–1385
44. Klee, C. B., Ren, H., and Wang, X. T. (1998) *J. Biol. Chem.* **273,** 13367–13370
45. Rusnak, F., and Mertz, P. (2000) *Physiol. Rev.* **80,** 1483–1521